Two interacting charged particles in an Aharonov-Bohm ring: Bound state transitions, symmetry breaking, persistent currents, and Berry's phase

Konstantinos Moulopoulos* and Martha Constantinou
University of Cyprus, Department of Physics, P.O. Box 20537, 1678 Nicosia, Cyprus
(Received 29 June 2004; revised manuscript received 1 November 2004; published 20 December 2004)

By using a Green's function procedure we determine exactly the energy spectrum and the associated eigenstates of a system of two oppositely charged particles interacting through a contact potential and moving in a one-dimensional ring threaded by a magnetic flux. Critical interactions for the appearance of bound states are analytically determined and are viewed as limiting cases of many-body results from the area of interaction-induced metal-insulator transitions in charged quantal mixtures. Analytical expressions on one-body probability and charge current densities for this overall neutral system are derived and their single-valuedness leads to the possibility of states with broken symmetry, with possible experimental signatures in exciton spectra. Persistent currents are analytically determined and their properties investigated from the point of view of an interacting mesoscopic system. A cyclic adiabatic process on the interaction potential is also identified, with the associated Berry's phase directly linked to the electric (persistent) currents, the probability currents having no contribution for a neutral system.

DOI: 10.1103/PhysRevB.70.235327 PACS number(s): 73.23.Ra, 71.35.Ji, 03.65.Vf, 03.65.Ge

I. INTRODUCTION

Quantum correlations in systems of interacting charged particles moving in nonsimply connected spaces and in the presence of Aharonov-Bohm fluxes is an especially important topic in condensed matter physics. It is still a wide-open area for both experimental and theoretical discoveries. In the present work a simple model problem of this type is exactly solved and some interesting properties are revealed that are associated with the interplay of interactions, topology (double-connectedness), and the characteristics of a charged mixture. These properties are exact and are determined in closed analytical forms.

The model problem consists initially of a neutral system of two interacting charged particles moving in a one-dimensional ring, threaded by a magnetic flux, and with a contact interaction. It is a model that can be applied, for example, to a system of an electron and a hole moving in an Aharonov-Bohm ring of sufficiently small size and at sufficiently low temperatures so that full quantum coherence around the ring has been established and the Aharonov-Bohm effect is fully operational. However, some generalizations are also made at the end of this paper to a non-neutral system and to higher dimensionality.

Magnetic field effects on electron-hole systems in a nanoring have recently been studied both theoretically[1–7] and experimentally.[8,9] Manifestations of the Aharonov-Bohm effect[10] in ring geometry are well known[11] at the single-particle level: the physical origin of the flux sensitivity of the state of a single particle in a quantum ring is its charge and its coupling to the vector potential. This coupling to the flux will consequently have opposite signs for two oppositely charged particles, i.e., an electron and a hole. An exciton, for instance, being a bound state of an electron and a hole, hence a neutral entity, is not sensitive to the flux as a whole, and this is demonstrated in the free-particle behavior of its center of mass. Such sensitivity of the Aharonov-Bohm type, however, *does* appear in the relative (internal) state and if this can be determined exactly it can give valuable information on an exciting topic in mesoscopic physics:[12,13] coexistence of Aharonov-Bohm effect with interparticle interactions. It can also serve as a model in effective two-particle theories of arbitrary many-body mixtures in Aharonov-Bohm configurations.

In this paper we follow a Green's function procedure in order to study such a simple two-particle system interacting with a contact potential and moving in such an Aharonov-Bohm ring. We solve the problem exactly, giving all possible eigenstates in closed analytical form, and determining the energy spectrum through a graphical procedure. Unlike previous works, we focus on the issue of possible bound states and we find critical interactions in closed form as functions of the magnetic flux and the center of mass angular momentum. Excited state energies are also investigated and an interesting pattern of discontinuities in the graphical solution is found with possible experimental consequences. We also examine carefully the issue of single-valuedness of measurable quantities, such as the probability and the charge current density, and present cases where energy lowering can occur with states that break the periodicity of the problem. This symmetry breaking is shown to lead to an interesting band-mode structure that has not been considered before in the exciton literature. Persistent currents for our interacting model system are analytically determined and their properties are investigated, especially with respect to variations of the magnetic flux and of the ring size. Comparisons are also made with the noninteracting behavior as well as with a rigorous upper bound known in the literature. In particular, a crossover is found for typical experimental values, where an attractive contact potential is shown to lead to enhanced conduction compared to the noninteracting case, for a sufficiently small ring radius. Finally, we generalize our model interaction by considering a theoretical process of slow variation of the interparticle interaction center and with

 ©2004 The American Physical Society

a potential of arbitrary form. A cyclic adiabatic variation of this type is found to be characterized by a geometric Berry's phase[14] which, apart from the usual Aharonov-Bohm contribution, also involves a term directly proportional to the electric (and *not* the probability) current density. It is also shown that a contribution from the probability currents would only arise for a non-neutral system. These properties are briefly shown to have a higher generality and, with appropriate modifications, to apply to systems with a more general potential and higher dimensionality.

Section II defines the problem, presents the center of mass behavior, and then proceeds to formulate the more interesting relative problem in terms of an integral equation for the relative wave functions. Section III determines appropriate Green's functions through a matching procedure and compares with other methods in the literature, which are compatible with standard symmetry arguments in exciton physics. Section IV presents an exact condition that graphically determines the entire energy spectrum of the two-particle problem and focuses on the issue of possible bound state transitions. We find that the total angular momentum of the pair, in combination with the Aharonov-Bohm flux, plays a crucial role in determining the corresponding critical interactions for binding. The transitions are viewed as particular cases of interaction-induced metal-insulator transitions in a neutral system of two charged components, and the critical interactions determined here in closed form are shown to be compatible with earlier many-body results. Section V gives the corresponding eigenfunctions in closed analytical form and discusses their cusp and symmetry properties. Section VI takes up the issue of the exact form of measurable quantities, such as the probability and charge density, as well as the probability current and electric current density: a more careful analysis than usual stresses the difference of physical information contained in each. The imposition of single-valuedness on such quantities leads to the possibility of states that have not been earlier discussed in the exciton literature and that violate the usual periodicity or antiperiodicity properties of ordinary states. This introduces a band-mode structure with some interesting behaviors in both ground state energy lowering and excited state energy discontinuities with possible experimental consequences. Persistent currents for arbitrary interactions and arbitrary symmetry breaking parameters are analytically determined in Sec. VII, their properties are carefully studied, and comparisons are made with the noninteracting behavior and with a rigorous upper bound known in the literature. Section VIII presents a cyclic adiabatic process that leads to Berry's phases directly related to persistent currents, a result that is shown to also be valid for an arbitrary interaction. Further important extensions of our model system are also made in this section that clarify the connection between the geometric phase and the various currents. It is shown, for example, that this connection is valid for a charged mixture (it would be completely absent in a system of a single charged component). Section IX presents our conclusions and gives a discussion of our results in a more general context.

II. THE SYSTEM

For reasons of simplicity we consider two oppositely charged spinless particles of equal masses m moving along a circular one-dimensional ring of radius R, which is threaded by a magnetic flux Φ. The position of each particle is described by angular variables φ_1 and φ_2. The two particles interact through an interaction $U(\varphi_1-\varphi_2)$ which in this paper is taken as a contact interaction of the form $U\delta(\varphi_1-\varphi_2)$, with U a real constant (of either sign) with dimensions of energy.

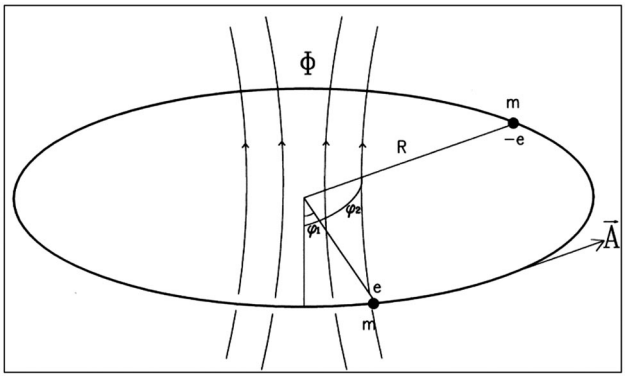

FIG. 1. Our model system and a choice of the vector potential $A=(\Phi/2\pi R)\hat{\varphi}$.

Although contacts are periodic in the relative variable $\varphi_1-\varphi_2$ with period 2π, we can always restrict values of this variable to the interval $(-\pi,\pi]$, in which case the interaction is simply of the above form (with just a single contact, for $\varphi_1-\varphi_2=0$, within this interval). The Schrödinger equation describing all the eigenfunctions $\Psi(\varphi_1,\varphi_2)$ of this system is

$$\left[\frac{1}{2m}\left(\frac{-i\hbar\partial_{\varphi_1}}{R}-\frac{e|\vec{A}|}{c}\right)^2+\frac{1}{2m}\left(\frac{-i\hbar\partial_{\varphi_2}}{R}+\frac{e|\vec{A}|}{c}\right)^2+U\delta(\varphi_1-\varphi_2)\right]\Psi(\varphi_1,\varphi_2)=E\Psi(\varphi_1,\varphi_2), \qquad (2.1)$$

where the most natural choice for the vector potential $\vec{A}$ is a vector tangential to every point of the circular ring with a constant magnitude $|\vec{A}|=\Phi/2\pi R$ (see Fig. 1).

The above equation can be decoupled if written in terms of center of mass (Φ_c) and relative (φ) variables (see Fig. 2), defined by

$$\Phi_c=\frac{\varphi_1+\varphi_2}{2}, \quad \varphi=\varphi_1-\varphi_2, \qquad (2.2)$$

and if $\Psi(\varphi_1,\varphi_2)$ is written as a product $\Psi_c(\Phi_c)\Phi(\varphi)$. Equation (2.1) then separates into two independent equations, one

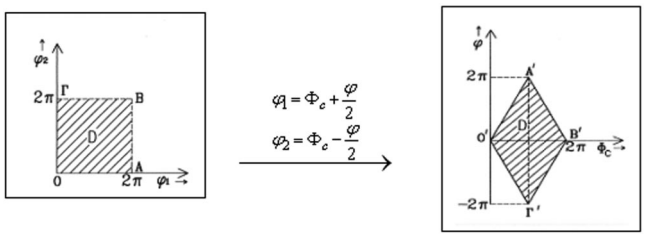

FIG. 2. Change of the original variables to center of mass and relative angular coordinates: the mapping of combined domains of definition is shown, which will be crucial for considerations of Sec. VI.

for each variable. The center of mass corresponds to a free uncharged particle with mass $2m$, namely

$$-\frac{\hbar^2}{4mR^2}\frac{d^2\Psi_c}{d\Phi_c^2}=E_c\Psi_c(\Phi_c), \tag{2.3a}$$

while the relative system corresponds to a charged particle with mass equal to the reduced mass $(m/2)$ of the system and subject to the interaction $U\delta(\varphi)$ as well as the minimal substitution, namely

$$\left[\frac{1}{m}\left(\frac{-i\hbar}{R}\frac{d}{d\varphi}-\frac{e|\vec{A}|}{c}\right)^2-(E-E_c)\right]\Phi(\varphi)=-U\delta(\varphi)\Phi(\varphi). \tag{2.3b}$$

In (2.3a) and (2.3b) E_c and Ψ_c are the energy and eigenfunctions of the center of mass, while E is always the total energy of the two-particle system. The solutions of (2.3a) are easy to find and are given in normalized form by

$$\Psi_c(\Phi_c)=\frac{1}{\sqrt{2\pi}}\exp\left(i\sqrt{\frac{4mR^2E_c}{\hbar^2}}\Phi_c\right), \tag{2.4}$$

where the allowed energies E_c can be determined by the requirement that all wave functions are single-valued when Φ_c changes by an integral multiple of 2π. This leads to the energy spectrum

$$E_c=\frac{\hbar^2N^2}{4mR^2} \tag{2.5}$$

with N being an *integer* ($\hbar N$ being the total angular momentum of the pair), the eigenstates then taking the simple form

$$\Psi_c(\Phi_c)=\frac{1}{\sqrt{2\pi}}e^{iN\Phi_c}. \tag{2.6}$$

It should be noted at the outset that the usual imposition of single-valuedness on the wave functions is not entirely rigorous although it leads to the correct results. A more proper argument should be based on single-valuedness of measurable quantities such as the probability density $\rho(\Phi_c)$ or the probability current density $J(\Phi_c)$ and such a more careful treatment will actually be given later for the relative problem. In the case of the center of mass states, if one considers, for instance, a linear combination of two states of the form (2.6), namely

$$\Psi_c(\Phi_c)=C_1e^{iN_1\Phi_c}+C_2e^{iN_2\Phi_c}$$

but with the corresponding N_1 and N_2 being arbitrary real numbers, then $\rho(\Phi_c)$ turns out to be

$$\rho(\Phi_c)=|C_1|^2+|C_2|^2+2\ \mathrm{Re}[C_1C_2^*e^{i(N_1-N_2)\Phi_c}] \tag{2.7}$$

and imposition of single-valuedness on $\rho(\Phi_c)$ leads to the condition that N_1-N_2 should be an integer. An additional assumption then that the state $\Psi_c=\mathrm{const}$ is an allowed solution (corresponding to $N=0$) leads finally to the condition that all N_i's must be integers. This more rigorous argument therefore gives an indirect justification for the easier standard approach based on wave functions.

The relative problem described by (2.3b) contains most of the interesting physics associated with possible bound state transitions and symmetry breakings and incorporates the influence of the center of mass on the internal behavior of the pair through the presence of E_c (and the associated integer N). In what follows, we will study (2.3b) through the method of Green's functions.

First, it is more convenient to write (2.3b) in a different form, namely

$$\left[\left(-i\frac{d}{d\varphi}-f\right)^2-B\right]\Phi(\varphi)=-\frac{U}{\Delta}\delta(\varphi)\Phi(\varphi), \tag{2.8}$$

which defines the following important quantities: $\Delta=\hbar^2/mR^2$ that will later be used as our energy unit, $B=E/\Delta-N^2/4$, a dimensionless form for the internal pair energy, and $f=\Phi/\Phi_0$, the so-called reduced flux, with $\Phi_0=hc/e=4.14\times10^{-15}T\ \mathrm{m}^2$, the magnetic flux quantum. (Note that we can restrict ourselves to the range $0\leqslant f<1$ because of the expected Aharonov-Bohm periodicity[11,15,16] of all properties with respect to f with period 1.) Equation (2.8) can be viewed as an inhomogeneous differential equation and has a solution that can be written in integral form, namely

$$\Phi(\varphi)=\int_{-\pi}^{\pi}d\varphi'G(\varphi,\varphi')\frac{U}{\Delta}\delta(\varphi')\Phi(\varphi'), \tag{2.9}$$

where an appropriate Green's function for this problem should satisfy

$$\left[\left(-i\frac{d}{d\varphi}-f\right)^2-B\right]G(\varphi,\varphi')=-\delta(\varphi-\varphi') \tag{2.10}$$

and will be determined in the next section, after the issue of imposition of appropriate boundary conditions is addressed rather carefully. We note that, although (2.9) is actually an integral equation for $\Phi(\varphi)$, nevertheless the solution can easily be found due to the δ-function form of our model interaction.

III. SYMMETRY PROPERTIES AND GREEN'S FUNCTION PROCEDURE

The appropriate Green's function $G(\varphi,\varphi')$ to be used in (2.9) must satisfy the defining equation (2.10), as well as the same boundary conditions that must be imposed on $\Phi(\varphi)$ at the ends of the interval $(-\pi,\pi]$. In order to see which type of boundary conditions is appropriate for this problem, it is advantageous at this point to temporarily extend the definition of the relative variable φ to the entire real line $(-\infty,\infty)$ and follow a line of approach that is based on a standard argument from the exciton literature. In this way we can exploit the 2π periodicity of contacts with respect to the relative variable and therefore draw conclusions about the symmetry properties of relative wave functions when these are viewed as functions on the entire real line. At the end, this will impose the proper boundary conditions that we need at the ends of our interval $(-\pi,\pi]$. It should be emphasized, however, that later, in Sec. VI, this standard argument will need

to be generalized to states that break these usual symmetry properties; this will be taken into account in anticipation even in the present section, where the most general mixed boundary conditions will actually be used [see below, Eq. (3.7)].

Following initially the standard approach[1] we first set

$$\Phi(\varphi) = e^{if\varphi}\chi(\varphi)$$

in (2.8), so that $\chi(\varphi)$ satisfies

$$\left(\frac{d^2}{d\varphi^2} + B\right)\chi(\varphi) = \frac{U}{\Delta}\delta(\varphi)\chi(\varphi),$$

and then we exploit the fact that, for $-\infty < \varphi < \infty$, $U(\varphi)$ is periodic in φ with period 2π. The functions $\chi(\varphi)$ must therefore have the Bloch form,[1] namely

$$\chi(\varphi) = e^{iq\varphi}u(\varphi) \quad \text{with } u(\varphi + 2\pi) = u(\varphi), \tag{3.1}$$

where q is a real dimensionless number (the analog of "crystal momentum") that lies within the first Brillouin zone $(-\pi/2\pi, \pi/2\pi]$, namely

$$-\tfrac{1}{2} < q \leqslant \tfrac{1}{2}. \tag{3.2}$$

The usual argument then involves the total wave functions $\Psi(\varphi_1, \varphi_2) = \Psi_c(\Phi_c)e^{if\varphi}\chi(\varphi)$ written in terms of the original angular variables. Combining (3.1) with (2.6) and (2.2) we obtain

$$\begin{aligned}\Psi(\varphi_1, \varphi_2) &\sim e^{iN[(\varphi_1+\varphi_2)/2]}e^{if(\varphi_1-\varphi_2)}e^{iq(\varphi_1-\varphi_2)}u(\varphi_1 - \varphi_2) \\ &= e^{i[(N/2)+f+q]\varphi_1}e^{i[(N/2)-f-q]\varphi_2}u(\varphi_1 - \varphi_2).\end{aligned} \tag{3.3}$$

The standard argument then imposes the requirement that the total wave function (3.3) must be single-valued with respect to φ_1 and φ_2 *independently*, hence periodic with respect to φ_1 and φ_2, each with period 2π. This leads to the independent conditions

$$\frac{N}{2} + f + q = n_1, \quad \frac{N}{2} - f - q = n_2, \tag{3.4}$$

with n_1 and n_2 arbitrary (and uncorrelated) integers. Adding and subtracting the two conditions finally leads to N: an integer (as seen earlier) and $f+q$=half integer or $f+q=n/2$, with n: an integer, with the observation that the integers N and n should be of the same type, either both even or both odd (this follows from $N=n_1+n_2$ and $n=n_1-n_2$ and will be used repeatedly in later sections). But the most important conclusion of this section is drawn from a combination with (3.1) which simply leads to

$$\Phi(\varphi) = e^{i(n/2)\varphi}u(\varphi) \tag{3.5}$$

with $u(\varphi)$ being 2π-periodic and n being an integer (of the same type as the center of mass integer N). This describes the usual symmetry properties of relative states: they are 4π-periodic, and they can be either 2π-periodic (for n even) or 2π-antiperiodic (for n odd). At the same time we can now go back to our interval $(-\pi, \pi]$ and see that, because of (3.5), the appropriate boundary conditions that we need to impose on $\Phi(\varphi)$ are mixed, and of the following type:

$$\Phi(\pi) = e^{in\pi}\Phi(-\pi) \text{ and } \Phi'(\pi) = e^{in\pi}\Phi'(-\pi), \tag{3.6}$$

where $\Phi'(\varphi)$ denotes the derivative $d\Phi/d\varphi$. Correspondingly, these are the boundary conditions that the Green's function $G(\varphi, \varphi')$, viewed as a function of φ only, should also satisfy.

We have, however, already warned the reader that single-valuedness arguments for wave functions are not entirely rigorous, and that more general considerations (based on measurable quantities) will be made later in Sec. VI. As a result, more general boundary conditions than (3.6) will emerge, and will be of the form

$$\Phi(\pi) = e^{i\theta}\Phi(-\pi), \quad \Phi'(\pi) = e^{i\theta}\Phi'(-\pi) \tag{3.7}$$

with θ an arbitrary real number (which we will later set to $\theta = n\pi + \vartheta$, with ϑ accounting for deviations from the ordinary case). For reasons of economy, we will now use these more general conditions in determining the appropriate Green's function for this problem, and we will have in mind that ordinary states will correspond to the special case $\theta = n\pi$. What remains for this section is the finding of $G(\varphi, \varphi')$ that solves (2.10) for $-\pi < \varphi, \varphi' \leqslant \pi$, under boundary conditions that are dictated by (3.7). A mathematical procedure leading to relevant matching conditions on $G(\varphi, \varphi')$ is presented in detail in Appendix A. It is then a tedious but rather straightforward exercise to find that imposition of (A1), (A5), and (A6) on the forms (A3) and (A4) finally results in the following Green's function:

$$G(\varphi, \varphi') = \left\{ \begin{array}{ll} \dfrac{e^{-i(\theta/2)}e^{i(f+\sqrt{B})(\pi+\varphi-\varphi')}}{4\sqrt{B}\,\sin\left[\pi(f+\sqrt{B}) - \dfrac{\theta}{2}\right]} - \dfrac{e^{-i(\theta/2)}e^{i(f-\sqrt{B})(\pi+\varphi-\varphi')}}{4\sqrt{B}\sin\left[\pi(f-\sqrt{B}) - \dfrac{\theta}{2}\right]}, & \varphi \leqslant \varphi' \\ \dfrac{e^{i(\theta/2)}e^{-i(f+\sqrt{B})(\pi+\varphi'-\varphi)}}{4\sqrt{B}\,\sin\left[\pi(f+\sqrt{B}) - \dfrac{\theta}{2}\right]} - \dfrac{e^{i(\theta/2)}e^{-i(f-\sqrt{B})(\pi+\varphi'-\varphi)}}{4\sqrt{B}\,\sin\left[\pi(f-\sqrt{B}) - \dfrac{\theta}{2}\right]}, & \varphi \geqslant \varphi' \end{array} \right\}, \tag{3.8}$$

which will later be used in (2.9) in order to give all relative eigenstates (the ordinary ones corresponding to $\theta=n\pi$, n: an integer of the same type as N).

For comparison with other methods[3] it should be noted that an alternative series method could be used for derivation of (3.8), provided that one is restricted to ordinary (periodic or antiperiodic) states. A Fourier transformation of (2.10) leads to a series representation of the form

$$G(\varphi,\varphi')=\frac{1}{2\pi}\frac{\hbar^2}{mR^2}\sum_{n=-\infty}^{\infty}\frac{e^{i(n/2)(\varphi-\varphi')}}{E-\frac{\hbar^2N^2}{4mR^2}-\frac{\hbar^2}{mR^2}\left(\frac{n}{2}-\frac{\Phi}{\Phi_0}\right)^2}, \tag{3.9}$$

which, upon changing integers to $N=n_1+n_2$ and $n=n_1-n_2$ and for a fixed center of mass quantum number N, yields

$$G(\varphi,\varphi')=\frac{\Delta}{2\pi}\sum_{n_1=-\infty}^{\infty}\frac{\exp\left[i\left(n_1-\frac{N}{2}\right)(\varphi-\varphi')\right]}{E-E_{n_1}^{(e)}-E_{n_2}^{(h)}}, \tag{3.10}$$

where $E_l^{(e)}=(\hbar^2/2mR^2)(l-f)^2$ and $E_l^{(h)}=(\hbar^2/2mR^2)(l+f)^2$ are separate single-particle energies of an electron and a hole, respectively, and $f=\Phi/\Phi_0$. The sum (3.10) can actually be evaluated with appropriate use of the complex plane and residue calculus to derive directly the relative wave functions [through (2.9)]. This is carried out in Appendix B [see Eq. (B2)] and is used in later sections [Eq. (5.2)].

IV. ENERGY SPECTRUM AND BOUND STATE TRANSITIONS

Let us first use our result (3.8) in order to obtain a closed form for the relative eigenstates. Substitution into (2.9) yields

$$\Phi(\varphi)=\frac{U}{\Delta}\Phi(0)[G_R(\varphi,0)\Theta(\varphi)+G_L(\varphi,0)\Theta(-\varphi)], \tag{4.1}$$

where $\Theta(\varphi)$ is the Heaviside step function, and

$$G_L(\varphi,0)=\frac{e^{-i(\theta/2)}e^{i(f+\sqrt{B})(\pi+\varphi)}}{4\sqrt{B}\sin\left[\pi(f+\sqrt{B})-\frac{\theta}{2}\right]}-\frac{e^{-i(\theta/2)}e^{i(f-\sqrt{B})(\pi+\varphi)}}{4\sqrt{B}\sin\left[\pi(f-\sqrt{B})-\frac{\theta}{2}\right]},$$

$$G_R(\varphi,0)=\frac{e^{i(\theta/2)}e^{-i(f+\sqrt{B})(\pi-\varphi)}}{4\sqrt{B}\sin\left[\pi(f+\sqrt{B})-\frac{\theta}{2}\right]}-\frac{e^{i(\theta/2)}e^{-i(f-\sqrt{B})(\pi-\varphi)}}{4\sqrt{B}\sin\left[\pi(f-\sqrt{B})-\frac{\theta}{2}\right]}. \tag{4.2}$$

This closed form of relative eigenfunctions will be modified to more convenient and transparent expressions in later sections [i.e., see (5.1), for $\theta=n\pi$] ; what we will be focusing on here is its use to derive a condition that will give the entire energy spectrum of the problem. Indeed by taking the limit $\varphi\to 0$ in (4.1) and by canceling the constant $\Phi(0)$ from both sides, we obtain after some trigonometric manipulations the following result:

$$\frac{\sin[2\pi\sqrt{B}]}{\cos[2\pi f-\theta]-\cos[2\pi\sqrt{B}]}=\frac{2\Delta\sqrt{B}}{U} \tag{4.3}$$

with $B=E/\Delta-N^2/4$. This is an exact and general condition that will provide the whole set of allowed energies $\{E\}$ of this two-particle problem. (We remind the reader that the arbitrary real parameter θ can be set to $\theta=n\pi+\vartheta$, with ϑ accounting for deviations from ordinary states). It should be noted that in Appendix B an alternative series method is outlined that applies to the case of ordinary states ($\theta=n\pi$) and that leads to a slightly different result, namely

$$\frac{\sin[2\pi\sqrt{B}]}{\cos[2\pi f+\pi N]-\cos[2\pi\sqrt{B}]}=\frac{2\Delta\sqrt{B}}{U}. \tag{4.4}$$

This is an alternative exact condition that will provide the energy spectrum, and since it has been derived by a different method it needs to be compared with our result (4.3). It is easy to see that, indeed, in the case of ordinary states ($\theta=n\pi$) (4.3) and (4.4) are equivalent, because n and N must be of the same type (either both even or both odd) as discussed in Sec. III. An analogous equivalence will also be shown about the eigenstates in the next section [Eqs. (5.1) and (5.2)]. However, it will be seen that expressions of the type of (4.4) that contain the center of mass quantum number N rather than the relative quantum number n involve the risk of obtaining wrong results when asymptotic limits are taken—for the limit $U\to 0$, for instance, (4.4) would give

$$E=\frac{\hbar^2}{mR^2}\left(f+\frac{N}{2}\right)^2+\frac{\hbar^2N^2}{4mR^2}$$

and *not* the correct

$$E=\frac{\hbar^2}{mR^2}\left(f-\frac{n}{2}\right)^2+\frac{\hbar^2N^2}{4mR^2}$$

that (4.3) gives for $\theta=n\pi$. Besides, the method of matching that we followed here is more general, as it allows for the possibility of $\theta\neq n\pi$ as we already saw in Sec. III. We proceed therefore with the use of (4.3) to determine graphically the energy spectrum of our model system.

Let us focus for this and the next section on the ordinary case $\theta=n\pi$ (periodic or antiperiodic states in the interval $(-\pi,\pi]$). Furthermore, since we are mostly interested in bound states we will only deal with an attractive interaction ($U<0$). [It is easy to see that (4.3) does not provide any bound energies (i.e., $E/\Delta<N^2/4$) when $U>0$, but only scattering states, which can of course also be found through the same graphical procedure that follows.]

Let us first start with the case $N=0$ (constant center of mass wave function and vanishing total angular momentum)

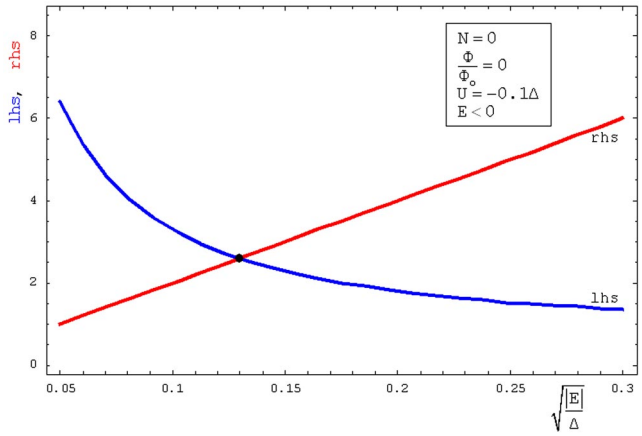

FIG. 3. (Color online) Graphical solution of the self-consistency condition for bound energy in the absence of magnetic flux.

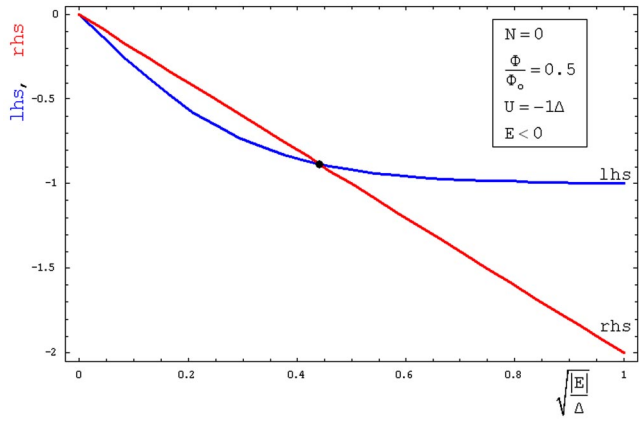

FIG. 4. (Color online) Graphical solution of the self-consistency condition for bound energy in the presence of magnetic flux.

and examine the differences in behavior between a flux-free and an $f \neq 0$ case. For $f=0$ we obtain from (4.3)

$$\cot\left[\pi\sqrt{\frac{E}{\Delta}}\right] = \frac{2\Delta}{U}\sqrt{\frac{E}{\Delta}}, \tag{4.5}$$

which for $U=-|U|$ and $E<0$ reads

$$\coth\left[\pi\sqrt{\frac{|E|}{\Delta}}\right] = \frac{2\Delta}{|U|}\sqrt{\frac{|E|}{\Delta}} \tag{4.6}$$

and a graphical representation of its left- and right-hand side (denoted by lhs and rhs, respectively) is given in Fig. 3. We find one and only one intersection, which determines the energy of the only bound state. This exists irrespective of the weakness of the attractive interaction, and it has to do with the fact that the lhs of (4.6) diverges at the origin (something that will change when we include a magnetic flux). In experiments with nanorings,[4,17] with a typical radius of 20 nm, with an effective mass $m^* \approx 0.067 m_e$ and dielectric constant $\varepsilon \approx 12.4$ (in GaAs/AlGaAs), the ground state energy is found to be $|E_0| \sim 13$ meV. This value is actually consistent with the above rough model: if we choose $|U|$ as a characteristic Coulomb energy, namely $|U| = e^2/2\varepsilon x_0$ with x_0 taken as a characteristic length of a one-dimensional hydrogen atom[18] which is $x_0 = a_0^*/2$, with the effective Bohr radius being $a_0^* = \varepsilon\hbar^2/m^* e^2 \simeq 97.9$ Å, then $U \approx -11.85$ meV. Using this value in (4.6) together with an effective $\Delta^* = \hbar^2/m^* R^2 \simeq 2.84$ meV we find that the bound state solution of (4.6) is $E_b = -12.37$ meV, a value very close to the experimental one.[4]

In the limit of large R ($R \gg \hbar/\sqrt{m|U|}$ and also $|E|/\Delta \gg 1$), a Taylor expansion of (4.6) around $1/R^2 \sim 0$ yields

$$E_{\text{ground}} \to -\frac{U^2}{4\Delta}(1 + 4\, e^{-\pi(|U|/\Delta)}). \tag{4.7}$$

The first term of (4.7) is the energy of a particle of mass $m/2$ that is bound on a potential $-R|U|\delta(x-x_0)$ in infinite one-dimensional straight line, and the second term can be viewed as a correction due to curvature, which in this limit ($|U| \gg \Delta$) decays exponentially fast.

Inclusion of a nonvanishing center of mass angular momentum ($N \neq 0$) yields in the limit $|E/\Delta - N^2/4| \gg 1$ the following ground state energy:

$$E^N_{\text{ground}} \to \frac{\hbar^2 N^2}{4mR^2} - \frac{U^2}{4\Delta}(1 + 4\cos[\pi N] e^{-\pi(|U|/\Delta)}) \tag{4.8}$$

that, apart from the center of mass kinetic energy, shows the manner in which the relative (internal) problem is affected by the motion of the pair as a whole.

It should be noted that the existence of a bound state in the case $N \neq 0$ is not always guaranteed, a point to which we shall return after we discuss the $f \neq 0$ case [see (4.10)].

Let us now include the Aharonov-Bohm flux ($f \neq 0$, or generally $f \neq$ integer, but we can always restrict values to $0 \leqslant f < 1$) and see the important qualitative differences with the above case. Since the left-hand side of (4.3) no longer diverges (in fact it vanishes) at the origin, an intersection is not guaranteed (even for $N=0$); its existence depends on a comparison between the slope of lhs and the slope of rhs at the origin. The former is $2\pi/(\cos[2\pi f]-1)$ (for $N=0$) and the latter is $2\Delta/U$, and an intersection (and therefore a bound state) exists only if $U \leqslant U_{\text{critical}}$ with

$$U_{\text{critical}} = -\frac{\Delta}{\pi}(1 - \cos[2\pi f]). \tag{4.9}$$

A bound state (for $N=0$) exists only if the attraction is sufficiently strong (and this is determined by the Aharonov-Bohm flux) and such a case is shown in Fig. 4. Generally speaking, the presence of f makes it more difficult to have a bound state, the worst case being for $f=1/2$. The existence of a critical interaction is a reflection of the competition between the effect of the magnetic field (that drives the two oppositely charged particles in opposite senses) and the attractive interaction (that drives the particles to cluster together). It is interesting to see, however, that if $U < -2\Delta/\pi$, then we always have binding irrespective of the value of f.

For $E>0$ and $N=0$, the lhs of (4.3) diverges at two points within the interval $[0,1)$, namely at $\sqrt{B}=f$ and $\sqrt{B}=1-f$, and these two converge into a single divergence when $f=1/2$, which is shown in Fig. 5 with an intersection corresponding

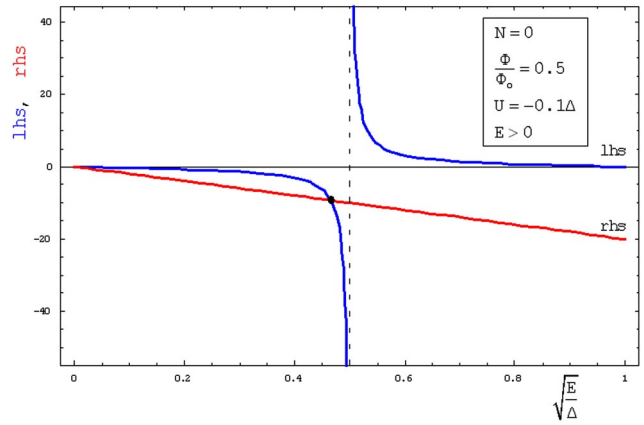

FIG. 5. (Color online) An example of the graphical solution for the energy spectrum of excited states: a special case of merged divergences (see Fig. 11 for a case that these divergences separate).

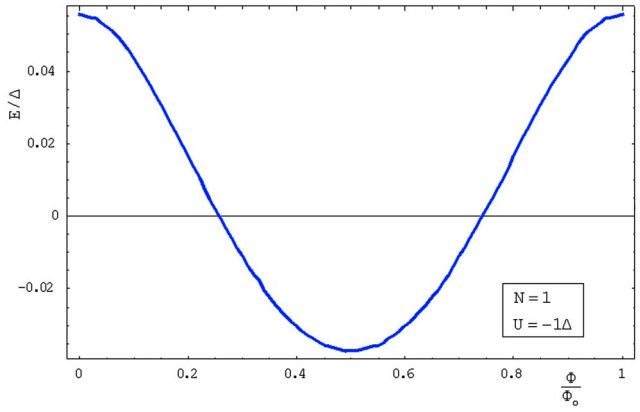

FIG. 6. (Color online) Ground state energy as a function of Aharonov-Bohm flux with both negative and positive energies.

to an excited state ($E>0$), one of the infinite ones that exist on the right (the pattern of divergences repeats itself for $E>\Delta$). It should be noted that these excited states can exhibit discontinuities whenever two divergences converge into a single one and this can have experimental consequences as will be discussed in Sec. VI.

For the case of $N\neq 0$ and arbitrary f one can show, again by comparison of slopes, that there is a critical interaction

$$U_{\text{critical}} = -\frac{\Delta}{\pi}(1-\cos[2\pi f+\pi \mathrm{N}]) \tag{4.10}$$

below which we have binding (now in the sense that $E<\Delta N^2/4$, i.e., with respect to the center of mass energy). This reproduces the ever-existence of a bound state for $f=0$ and N: even, as well as (4.9) for $f\neq 0$. It is interesting that for N: odd, we have a nonvanishing U_{critical} (hence more difficult binding) even for the flux-free case (while for $f=1/2$, it is the N: even case that produces a nonzero U_{critical}). It seems that the symmetry of the center of mass wave function and the type of the associated angular momentum plays a major role on the binding of the pair. These factors also play a role in the appearance of discontinuities of excited state energies with possible experimental consequences, as we will see later in Sec. VI. It is interesting also to note that for general N, it is possible to even have $E<0$ for the range of values of f where

$$\frac{U}{\Delta} < \frac{N}{\sinh[\pi N]}(\cos[2\pi f+\pi N]-\cosh[\pi N])$$

is valid. Such an example is given for $N=1$ in Fig. 6.

Although this problem of two interacting particles is exactly soluble and the transition from an excited to a bound state can be easily seen through the above graphical solution, it would be instructive to compare with a many-body criterion[19] from the area of interaction-induced metal-insulator transitions in charged quantal mixtures: the analytic behavior of the energy as a function of f should also determine the point of the transition according to the following procedure. We write the lowest excited state energy in the form $B=Cf^2$ and we look at the analytical behavior of C as a function of f in the limit $f\to 0$ (to be taken at the end). At the point where C vanishes we should have a transition from an excited state (the analog of the metallic state) to a bound state (the analog of an insulating state). Let us look, for example, at the case $N=0$ and the lowest excited state energy with $E^0>0$ (always for $U<0$ and $f\neq 0$). Equation (4.3) now reads

$$\frac{\sin\left[2\pi\sqrt{\frac{E^0}{\Delta}}\right]}{\cos[2\pi f]-\cos\left[2\pi\sqrt{\frac{E^0}{\Delta}}\right]} = \frac{2\Delta\sqrt{\frac{E^0}{\Delta}}}{U} \tag{4.11}$$

and cannot be solved analytically to obtain $E^0(f)$, but it can provide the necessary information through the graphical procedure: If we had a noninteracting system ($U\to 0^-$) then the straight line of the rhs would be vertical pointing downwards, and the first intersection point would therefore be at

$$\sqrt{\frac{E^0}{\Delta}} = f.$$

Hence, in this limiting case we would obtain $E^0=\Delta f^2$ (which agrees with the result[19] $E=(e^2/mc^2)A^2$ for noninteracting particles) and, naturally, the coefficient Δ never vanishes, as expected (no transition for $U=0$).

If we now turn on a small $U<0$, we can determine the lowest correction to the above trivial result, namely the small displacement of the intersection point away from the above value f. By following a Taylor expansion of (4.11) in the neighborhood of $\sqrt{E/\Delta}\sim f$ and solving with respect to E, we obtain

$$E^0 \simeq \Delta\left(f+\frac{U}{\pi(-4\Delta f+U\cot[2\pi f])}\right)^2. \tag{4.12}$$

If this is further expanded in powers of U, and if the result is written in the form $E^0=Cf^2$, we finally obtain that the coefficient C vanishes whenever

$$U_{\mathrm{cr}} = -2\pi\Delta f^2 + \frac{2}{3}\Delta\pi^3 f^4 + \cdots . \tag{4.13}$$

This indeed agrees with our earlier result (4.9) for U_{critical}, if this is expanded with respect to f term by term.

We conclude that the value of the critical interaction that, for this soluble problem, has been determined exactly, is also compatible with another more general many-body criterion for the transition (that is valid also for insoluble problems of more than two particles).

We finally give the asymptotic form of the ground state energy in the general case $f \neq 0$, $N \neq 0$, for the limit of large radius. This turns out to be

$$E^N_{\mathrm{ground}} = \frac{\hbar^2 N^2}{4mR^2} - \frac{U^2}{4\Delta}(1 + 4\cos[2\pi f + \pi N]e^{-\pi(|U|/\Delta)}) \tag{4.14}$$

and it naturally generalizes (4.8). Apart from the role of the center of mass on the internal energy, we also observe the expected periodic dependence (Aharonov-Bohm oscillations) with respect to the magnetic flux with the period equal to the flux quantum Φ_0.

A final comment is that the energy values as a function of f are symmetric around $f=1/2$, where we have a maximum for N: even (in agreement with measurements in experiments with excitons) as shown in Fig. 7, and a minimum for N: odd (see Fig. 6). It is interesting to note that for $f=1/2$, we have the lowest binding for N: even and the highest binding energy for N: odd. This observation correlates well with our earlier conclusion on U_{critical} [Eq. (4.10)], as well as with some disconnectedness property of eigenfunctions that we shall see below (end of the next section). We will also see in Sec. VI that Figs. 6 and 7 can be viewed as special cases (shifted bands) of a band-mode structure that will be introduced later.

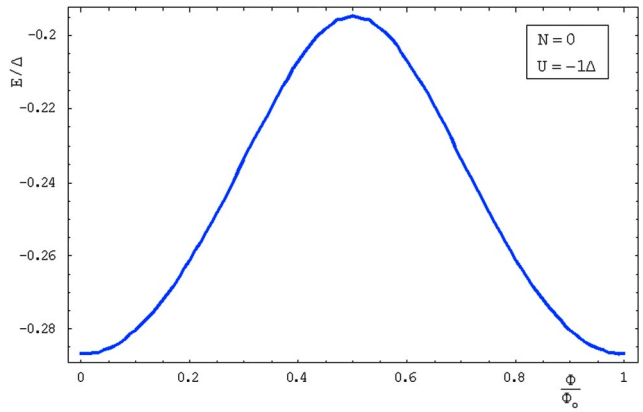

FIG. 7. (Color online) Similar to Fig. 6 but with a vanishing center of mass angular momentum.

V. SYSTEM EIGENFUNCTIONS

The entire set of eigenfunctions for the relative problem is given by (4.1) with the quantities G_R and G_L being defined by (4.2), a result that was based on the Green's function (3.8) and which is very general (for arbitrary θ). For the ordinary case $\theta = n\pi$, (4.1) yields

$$\Phi(\varphi) = \Phi(0)e^{if\varphi} \times \begin{cases} \dfrac{\exp\left[-2i\pi\left(f-\dfrac{n}{2}\right)\right]\sin[\sqrt{B}\varphi] - \sin[\sqrt{B}(\varphi-2\pi)]}{\sin[2\pi\sqrt{B}]}, & 0 \leqslant \varphi \leqslant 2\pi \\ \dfrac{-\exp\left[2i\pi\left(f-\dfrac{n}{2}\right)\right]\sin[\sqrt{B}\varphi] + \sin[\sqrt{B}(\varphi+2\pi)]}{\sin[2\pi\sqrt{B}]}, & -2\pi \leqslant \varphi \leqslant 0. \end{cases} \tag{5.1}$$

For comparison with the series method we note that Eq. (B2), in combination with the exact summation (B3), yields

$$\Phi(\varphi) = \Phi(0)e^{if\varphi} \times \begin{cases} \dfrac{\exp\left[-2i\pi\left(f+\dfrac{N}{2}\right)\right]\sin[\sqrt{B}\varphi] - \sin[\sqrt{B}(\varphi-2\pi)]}{\sin[2\pi\sqrt{B}]}, & 0 \leqslant \varphi \leqslant 2\pi \\ \dfrac{-\exp\left[2i\pi\left(f+\dfrac{N}{2}\right)\right]\sin[\sqrt{B}\varphi] + \sin[\sqrt{B}(\varphi+2\pi)]}{\sin[2\pi\sqrt{B}]}, & -2\pi \leqslant \varphi \leqslant 0, \end{cases} \tag{5.2}$$

which is equivalent to (5.1) because of the already announced fact that n and N are integers of the same type. In what follows we briefly discuss the general form and properties of these relative eigenstates.

First, for $f=0$ all states turn out to be real [we will always set $\Phi(0)=1$]. For the attractive potential ($U<0$) a typical form of the single bound state, for $N=0$, demonstrates a combination of a local exponential decrease (around $\varphi\sim 0$) with a 2π periodicity (valid for all N: even) and with no nodes. The behavior around $\varphi\sim 0$ is generally of the form

$$e^{-|\varphi|/\lambda_c} \tag{5.3}$$

with the characteristic angle λ_c determined by Taylor expansion of (5.1) that finally yields

$$\lambda_c = -\frac{2\Delta}{U}, \tag{5.4}$$

a result independent of N, f, and the actual value of the energy E. This is related to the cusp (discontinuity of derivative) at the origin, which can very generally be found to be $(U/\Delta)\Phi(0)$, and can be more generally shown at the level of the Schrödinger equation (2.8) without knowledge of the actual solutions. These findings generalize well-known results in infinite straight space.

For cases with $E>0$ (excited states) the wave functions have more nodes (they are oscillatory, apart from the cusp at the origin) and for a repulsive potential ($U>0$) the cusp has positive sign (making the wave function locally increasing for $\varphi\geqslant 0$).

Cases of nonzero N (both even and odd), again for an attractive potential, demonstrate the expected 2π periodicity for N: even and the 2π-antiperiodicity for N: odd, as well as the appropriate cusp in the neighborhood of $\varphi\sim 0$. For cases of $E>0$, we have more oscillatory behavior and in special cases where $E=\Delta(N^2/4)$ the states become linear, namely

$$\Phi(\varphi)=\Phi(0)\times\begin{cases}1-\dfrac{\varphi}{2\pi}, & \varphi\geqslant 0\\[2ex] 1+\dfrac{\varphi}{2\pi}, & \varphi\leqslant 0.\end{cases} \tag{5.5}$$

Finally, when we introduce a nonvanishing flux ($f\neq 0$), the relative wave functions now acquire an imaginary part. It can be shown that the imaginary part always has a continuous derivative at $\varphi\sim 0$, and the proper cusp $(U/\Delta)\Phi(0)$ appears only in the real part of the wave functions. It is interesting to note that in the special case $f=1/2$, the modulus of the wave functions becomes disconnected (it vanishes at $\pm\pi$) for even N (while for $f=0$ the same happens for odd values of N). It is actually easy to show that these cases are immediately related to $\cos[2\pi f+\pi N]=-1$ and hence, by (4.10), to cases of more difficult binding ($|U_{\text{critical}}|$ takes its maximum value $2\Delta/\pi$, and even in case of binding we observe the local maximum of Fig. 7). Again, these cases will be shown to correspond to the band edges of a band-mode structure introduced in the next section.

VI. BROKEN-SYMMETRY STATES

Let us now investigate the issue of single-valuedness of various measurable quantities and see if this can lead to cases of $\theta\neq n\pi$, namely to states that, under a change of the relative variable φ by $\pm 2\pi$, are neither periodic nor antiperiodic. We shall determine the most general form of four distinct one-body physical quantities: the probability density $\rho(\overline{\varphi})$, the electric charge density $\rho_{\text{el}}(\overline{\varphi})$, the probability current density $J(\overline{\varphi})$, and the electric current density $J_{\text{el}}(\overline{\varphi})$, where $\overline{\varphi}$ always denotes an angular variable on the physical circle that describes the point on the ring, where each quantity is locally determined. Since we have a system of more than one particle, each of the above quantities is given by the expectation value of an appropriate many-body operator with respect to a general two-particle state of our model system. The corresponding operators are defined by

$$\hat{\rho}(\overline{\varphi})=\sum_{i=1}^{N}\delta(\overline{x}-x_i)=\frac{1}{R}\sum_{i=1}^{N}\delta(\overline{\varphi}-\varphi_i), \tag{6.1}$$

$$\hat{\rho}_{\text{el}}(\overline{\varphi})=\sum_{i=1}^{N}q_i\delta(\overline{x}-x_i)=\frac{1}{R}\sum_{i=1}^{N}q_i\delta(\overline{\varphi}-\varphi_i), \tag{6.2}$$

$$\hat{J}(\overline{\varphi})=\frac{1}{2R}\sum_{i=1}^{N}\left(\frac{\hat{p}_i}{m_i}\delta(\overline{\varphi}-\varphi_i)+\delta(\overline{\varphi}-\varphi_i)\frac{\hat{p}_i}{m_i}\right)-\frac{\vec{A}(\overline{\varphi})}{Rc}\sum_{i=1}^{N}\frac{q_i}{m_i}\delta(\overline{\varphi}-\varphi_i), \tag{6.3}$$

$$\hat{J}_{\text{el}}(\overline{\varphi})=\frac{1}{2R}\sum_{i=1}^{N}q_i\left(\frac{\hat{p}_i}{m_i}\delta(\overline{\varphi}-\varphi_i)+\delta(\overline{\varphi}-\varphi_i)\frac{\hat{p}_i}{m_i}\right)-\frac{\vec{A}(\overline{\varphi})}{Rc}\sum_{i=1}^{N}\frac{q_i^2}{m_i}\delta(\overline{\varphi}-\varphi_i), \tag{6.4}$$

where $N=2$ for our case, $x_i=R\varphi_i$ is the position of the ith particle (of charge q_i and mass m_i) on the physical ring, and $\hat{p}_i$ denotes $-i\hbar(\partial/\partial x_i)=-(i\hbar/R)(\partial/\partial\varphi_i)$. The variables φ_i will become dummy integration variables in the expectation values to be evaluated below, so that, at the end, each quantity will depend on the absolute angular variable $\overline{\varphi}$ only. [The last terms of (6.3) and (6.4) have emerged from products of minimal couplings with delta functions, i.e., $[\hat{p}_i-(q_i/c)\boldsymbol{A}(x_i)]\delta(\overline{x}-x_i)$, and use of elementary δ-function properties.]

Note that in our case of $N=2$ and with $m_1=m_2=m$ and $q_1=-q_2=e$, there is an immediate connection of the probability current $\hat{J}$ with the electric charge density $\hat{\rho}_{\text{el}}$ [the last term of (6.3)], and of the electric current $\hat{J}_{\text{el}}$ with the probability density $\hat{\rho}$ [the last term of (6.4)], and these connections will be important in the following sections. The measurable quantities that correspond to the above operators, for an arbitrary two-particle state $|\Psi(\varphi_1,\varphi_2)\rangle$, would be given by appropriate expectation values with the use of φ_1, φ_2 as dummy variables, for instance

$$\rho(\overline{\varphi}) = \langle \Psi | \hat{\rho}(\overline{\varphi}) | \Psi \rangle = \int d\varphi_1 \int d\varphi_2 \Psi^*(\varphi_1, \varphi_2) \hat{\rho}(\overline{\varphi}) \Psi(\varphi_1, \varphi_2), \tag{6.5}$$

which would give an expected result, namely

$$\rho(\overline{\varphi}) = \frac{1}{R} \int d\varphi_2 |\Psi(\overline{\varphi}, \varphi_2)|^2 + \frac{1}{R} \int d\varphi_1 |\Psi(\varphi_1, \overline{\varphi})|^2 \tag{6.6}$$

for the probability density. (Integrals with respect to each φ_i are always understood to be from 0 to 2π.)

In a similar fashion, the remaining three quantities turn out to be

$$\rho_{\mathrm{el}}(\overline{\varphi}) = \frac{e}{R} \int d\varphi_2 |\Psi(\overline{\varphi}, \varphi_2)|^2 - \frac{e}{R} \int d\varphi_1 |\Psi(\varphi_1, \overline{\varphi})|^2 \tag{6.7}$$

for the electric charge density,

$$\begin{aligned} J(\overline{\varphi}) = {} & \frac{i\hbar}{2mR^2} \int d\varphi_2 \left[\Psi(\overline{\varphi}, \varphi_2) \frac{\partial \Psi^*(\overline{\varphi}, \varphi_2)}{\partial \overline{\varphi}} \right. \\ & \left. - \Psi^*(\overline{\varphi}, \varphi_2) \frac{\partial \Psi(\overline{\varphi}, \varphi_2)}{\partial \overline{\varphi}} \right] \\ & + \frac{i\hbar}{2mR^2} \int d\varphi_1 \left[\Psi(\varphi_1, \overline{\varphi}) \frac{\partial \Psi^*(\varphi_1, \overline{\varphi})}{\partial \overline{\varphi}} \right. \\ & \left. - \Psi^*(\varphi_1, \overline{\varphi}) \frac{\partial \Psi(\varphi_1, \overline{\varphi})}{\partial \overline{\varphi}} \right] - \frac{\hbar}{mR} \frac{\Phi}{\Phi_0} \frac{\rho_{\mathrm{el}}(\overline{\varphi})}{e} \end{aligned} \tag{6.8}$$

for the probability current density, and

$$\begin{aligned} J_{\mathrm{el}}(\overline{\varphi}) = {} & \frac{i\hbar e}{2mR^2} \int d\varphi_2 \left[\Psi(\overline{\varphi}, \varphi_2) \frac{\partial \Psi^*(\overline{\varphi}, \varphi_2)}{\partial \overline{\varphi}} \right. \\ & \left. - \Psi^*(\overline{\varphi}, \varphi_2) \frac{\partial \Psi(\overline{\varphi}, \varphi_2)}{\partial \overline{\varphi}} \right] \\ & - \frac{i\hbar e}{2mR^2} \int d\varphi_1 \left[\Psi(\varphi_1, \overline{\varphi}) \frac{\partial \Psi^*(\varphi_1, \overline{\varphi})}{\partial \overline{\varphi}} \right. \\ & \left. - \Psi^*(\varphi_1, \overline{\varphi}) \frac{\partial \Psi(\varphi_1, \overline{\varphi})}{\partial \overline{\varphi}} \right] - \frac{e\hbar}{mR} \frac{\Phi}{\Phi_0} \rho(\overline{\varphi}) \end{aligned} \tag{6.9}$$

for the electric current density, all quantities determined locally at $\overline{\varphi}$. [In the above we have again chosen $\boldsymbol{A}(\overline{\varphi}) = (\Phi/2\pi R)\hat{\varphi}$]. The slightly different structure of signs in these expressions will be essential for the results of the following sections. It is easy to verify that, in case of noninteracting particles [when $\Psi(\varphi_1, \varphi_2) = \Psi_1(\varphi_1)\Psi_2(\varphi_2)$] they can all be written as simple sums of separate single-particle contributions, i.e., of the form $\rho(\overline{\varphi}) = \rho_1(\overline{\varphi}) + \rho_2(\overline{\varphi})$, $J(\overline{\varphi}) = J_1(\overline{\varphi}) + J_2(\overline{\varphi})$, etc., as expected.

However, in order to reach useful conclusions on the interacting case, it is advantageous to change dummy variables to center of mass (Φ_c) and relative angular coordinates (φ) [see Eq. (2.2)], and this requires some care (see Fig. 2 where the proper combined variation of Φ_c and φ is shown). It is then a rather tedious exercise to show that (6.6)–(6.9) are transformed into more complex results that involve the familiar wave functions $\Psi_c(\Phi_c)$ and $\Phi(\varphi)$ of Sec. II. Examples of such expressions appear in Appendix C.

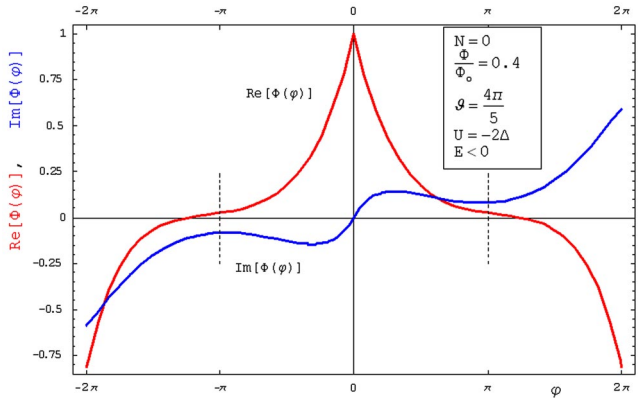

FIG. 8. (Color online) An example of a broken-symmetry state (with energy at the minima of Fig. 9).

Let us use these new expressions in examples of how one can reach conclusions associated with single-valuedness with respect to $\overline{\varphi}$. If one considers, for instance, linear combinations of center of mass eigenfunctions [such as in (2.6) with N_1, N_2 arbitrary real numbers] and of relative wave functions [such as in (3.5) but with n_1, n_2 again arbitrary real parameters], namely

$$\begin{aligned} \Psi(\Phi_c, \varphi) = {} & (Ae^{iN_1\Phi_c} + Be^{iN_2\Phi_c})(Ce^{i(n_1/2)\varphi} u_1(\varphi) \\ & + De^{i(n_2/2)\varphi} u_2(\varphi)) \end{aligned} \tag{6.10}$$

then the following observations can be made: The form (C1) remains invariant under $\overline{\varphi} \to \overline{\varphi} + 2\pi$ if

$$\left| \Psi_c\left(\overline{\varphi} \mp \frac{\varphi}{2}\right) \right|^2 = \left| \Psi_c\left(\overline{\varphi} \mp \frac{\varphi}{2} + 2\pi\right) \right|^2, \tag{6.11}$$

which leads to the requirement that $N_1 - N_2$ be an integer. This is actually a generalization of the argument following (2.7), and acceptance of the constant solution $N=0$ leads to the usual integer values for all N's. A more useful conclu-

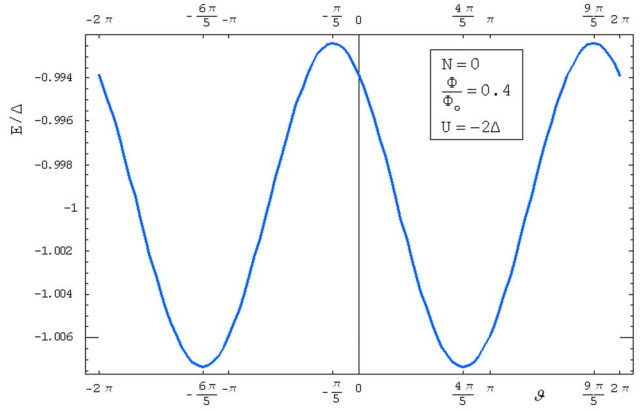

FIG. 9. (Color online) Effect of the symmetry breaking parameter on the bound state energy spectrum for a nontrivial choice of Aharonov-Bohm flux.

sion, however, comes from the form (C2) which is invariant under $\bar{\varphi} \to \bar{\varphi} + 2\pi$ when the modulus of the relative wave function $\Phi(\varphi)$ is 4π periodic, and use of (6.10) leads to the requirement that $n_1 - n_2$ be an integer; this does not, however, imply that each n_i should separately be an integer, as the value $n=0$ does not correspond to any special state that should necessarily be accepted [from (3.5) $n=0$ would just correspond to a 2π-periodic state and there is no physical reason to be restricted to such periodic relative states). Such a relative state, which breaks the symmetry of the problem, is shown in Fig. 8 (where Re denotes its real part and Im its imaginary part): in spite of the 4π periodicity of its modulus, there is a nontrivial phase difference that connects the values of the overall complex wave function at the two ends of our interval $(-\pi, \pi]$. This additional phase cannot be gauged away [it is directly linked to the reduced flux as will be seen below (i.e., Eq. (6.18)] and it is essentially a manifestation of the Aharonov-Bohm effect at the two-particle level. It is a measurable quantity and, as will be shown below, it directly affects other physical properties, such as the energy and the electric currents [as will be demonstrated later in Fig. 9 and in Eq. (6.28)].

Similar conclusions can be reached through the use of forms (C3) and (C4) for the probability current. The evidence is that the usual form (3.5) should permit noninteger values for n, or, alternatively, we could generalize it to

$$\Phi(\varphi) = e^{i(\theta/2\pi)\varphi} u(\varphi) \tag{6.12}$$

by introducing a general real angular parameter θ which can always be set to

$$\theta = n\pi + \vartheta, \; n\text{:integer}, \; \vartheta\text{: real} \tag{6.13}$$

with $\vartheta = 0$ accounting for the ordinary case described by (3.5). This freedom in the choice of ϑ has already been taken into account for the derivation of (3.8) and the relative eigenstates (4.1). The most general form of relative wave functions now turns out to be

$$\Phi(\varphi) = \Phi(0) e^{if\varphi} \times \begin{cases} \dfrac{e^{-2i\pi f} e^{i(\pi n + \vartheta)} \sin[\sqrt{B}\varphi] - \sin[\sqrt{B}(\varphi - 2\pi)]}{\sin[2\pi\sqrt{B}]}, & 0 \leqslant \varphi \leqslant 2\pi \\ \dfrac{-e^{2i\pi f} e^{-i(\pi n + \vartheta)} \sin[\sqrt{B}\varphi] + \sin[\sqrt{B}(\varphi + 2\pi)]}{\sin[2\pi\sqrt{B}]}, & -2\pi \leqslant \varphi \leqslant 0 \end{cases} \tag{6.14}$$

and generalizes the ordinary states given by (5.1). In fact it can be shown that (6.14) satisfies the relative Schrödinger equation (2.8) (with the appropriate cusp at $\varphi \sim 0$) independent of the value of ϑ, but giving a modified energy spectrum that is now given by

$$\frac{\sin[2\pi\sqrt{B}]}{\cos[2\pi f - n\pi - \vartheta] - \cos[2\pi\sqrt{B}]} = \frac{2\Delta\sqrt{B}}{U}. \tag{6.15}$$

This in fact is the condition (4.3) obtained at the beginning of Sec. IV [through the limit $\varphi \to 0$ and cancellation of the common factor $\Phi(0)$].

Let us now elaborate on this more general consideration. By going back to (3.3) it is straightforward to show that (6.12) implies

$$\Psi(\varphi_1 + 2\pi, \varphi_2) = \Psi(\varphi_1, \varphi_2) \exp\left[i\left(\frac{N}{2} + f + q \right) 2\pi \right],$$

$$\Psi(\varphi_1, \varphi_2 + 2\pi) = \Psi(\varphi_1, \varphi_2) \exp\left[i\left(\frac{N}{2} - f - q \right) 2\pi \right],$$

which are in turn simplified into

$$\Psi(\varphi_1 + 2\pi, \varphi_2) = \Psi(\varphi_1, \varphi_2) e^{i\vartheta}$$

and

$$\Psi(\varphi_1, \varphi_2 + 2\pi) = \Psi(\varphi_1, \varphi_2) e^{-i\vartheta}, \tag{6.16}$$

hence ϑ indeed accounts for the violation of the usual separate single-valuedness. Equation (6.16) can be derived from (3.7) [in combination with $\Phi(\varphi) = e^{if\varphi}\chi(\varphi)$ and (3.1)] that gives $e^{i\theta} = e^{2\pi i(f+q)}$, with q the "crystal momentum" of (3.1), which effectively yields (mod 2π)

$$\theta = 2\pi(f + q) \tag{6.17}$$

and

$$\vartheta = 2\pi\left(f + q + \frac{N}{2} \right) = 2\pi\left(f + q - \frac{n}{2} \right), \tag{6.18}$$

the last equality being valid because integers N and n are of the same type. [Equation (6.18) will be useful for the results and figures of the next section, if viewed as the definition of q with respect to physical quantities such as f, N, and ϑ]. With use of the above it is rather easy to show that (6.14) indeed satisfies the Bloch form (3.1): if $\Phi(\varphi)$ is written as $\Phi(\varphi) = e^{i(f+q)\varphi} u_{\pm}(\varphi) = e^{i(\theta/2\pi)\varphi} u_{\pm}(\varphi)$, it turns out that indeed

$$u_-(\varphi - 2\pi) = u_+(\varphi) \quad (\text{for } 0 \leqslant \varphi \leqslant 2\pi)$$

and

$$u_+(\varphi + 2\pi) = u_-(\varphi) \quad (\text{for } -2\pi \leqslant \varphi \leqslant 0),$$

showing that $u(\varphi)$ is always 2π periodic and demonstrating, therefore, the consistency of our approach.

It is interesting to note that our introduction of θ defines a band problem for the relative coordinate [see (3.7)], and this in turn induces separate band problems for each particle with a Bloch phase ϑ (when the physical circle is viewed as the unit cell). The usual imposition of separate single-valuedness [that led to (3.4)] is then a very special case that corresponds to the center ($\vartheta=0$) of each separate band. By returning then to (6.17) and (6.18) we also observe that this corresponds to $\theta=n\pi$ (as noted earlier) and to a very special value of the "relative crystal momentum," namely

$$q = -f - \frac{N}{2} \tag{6.19}$$

for ordinary states. These observations will be useful in understanding the behavior of energy, other measurable quantities, and the states themselves under the general broken-symmetry case in the results that follow, where we will see that other points of the "relative bands" (i.e., $q=0, \pm\frac{1}{2}$) are even more special and can lead to observable effects.

Consideration of such broken-symmetry states raises a plausible question: would a choice of $\vartheta \neq 0$ lead to energy gain? Let us examine whether introduction of a nonvanishing ϑ could lead to energy lowering compared to ordinary cases, and let us temporarily focus on bound states $[E<\Delta(N^2/4)]$ since this would be the most dramatic effect (symmetry breaking leading to stronger binding).

Starting from the new (and most general) condition for the energy spectrum (for bound states), namely Eq. (6.15) for $B<0$, we obtain

$$\frac{\partial E}{\partial \vartheta} = \frac{4\Delta^2(\sqrt{|B|})^3 \sin[2\pi f - \pi n - \vartheta]}{(U - 4\pi\Delta|B|)\sinh[2\pi\sqrt{|B|}] - 2\pi U\sqrt{|B|}\cosh[2\pi\sqrt{|B|}]} \tag{6.20}$$

[which will actually be related to $J_{\mathrm{el}}(\overline{\varphi})$ and also to the persistent currents below]. The local extrema of bound state energy can be found at values of ϑ where (6.20) vanishes, and this occurs whenever

$$\vartheta = 2\pi f + \pi N - k\pi \tag{6.21}$$

with k an integer. [Note from (6.18) that $k=-2q$, so this happens for $q=$integer$/2$, namely the edges or centers of the "relative bands."] Correspondingly the sign of

$$\frac{\partial^2 E}{\partial \vartheta^2} = -\frac{4\Delta^3(\sqrt{|B|})^5 \cos[k\pi]}{4\pi^2\Delta(\sqrt{|B|})^3\cos[k\pi] + (\pi|U| - \Delta)\cosh[2\pi\sqrt{|B|}]}$$

shows that these extrema are local minima whenever k is even (and maxima whenever k is odd). This is demonstrated in Fig. 9 for a nontrivial choice of f. The corresponding wave function (that breaks the symmetry with the energetically optimal value of ϑ) was earlier shown in Fig. 8.

It is instructive to classify these results from the point of view of the band-theoretic consideration advanced above. A combination of (6.18) and (6.20) shows that always $\partial E/\partial\vartheta \propto \sin[2\pi q]$ and $\partial^2 E/\partial\vartheta^2 \propto \cos[2\pi q]$, and that the ground state energy takes its minimal value for q: integer (or, within the First Brillouin Zone, for $q=0$, at the center of the "relative band") and becomes maximum for q: odd/2 (i.e., at the "relative band" edges). A typical ground state band is shown in Fig. 10. [We shall see below an alternating inversion of these roles for excited states ($B>0$) but with some superimposed discontinuity structure.] From this viewpoint, behaviors such as Fig. 6 or Fig. 7 are qualitatively equivalent to Fig. 10 (merely shifted) in view of (6.18). In case of absence of a magnetic flux, ordinary cases [described by (6.19)] correspond to minimum ground state energy only for N: even (and to a maximum for N: odd); the symmetry breaks in a nontrivial way only for an $f \neq$ integer$/2$, because it is those cases that the minimum ($q=0$) corresponds to nontrivial values of ϑ or θ (Fig. 9 shows such an example). It should also be noted that the ground state energy band $E(q)$ in the first Brillouin zone, although numerically determined, can always be fitted accurately with a simple sine or cosine function (see Fig. 10), with the position of the middle of the band and the bandwidth following behaviors which, in the case of strong $|U|$, follow patterns always consistent with (4.14): the band fluctuates around $-U^2/4\Delta+\Delta(N^2/4)$ and the bandwidth is $(2U^2/\Delta)e^{-\pi(|U|/\Delta)}$. Also, for the range of values of q for which

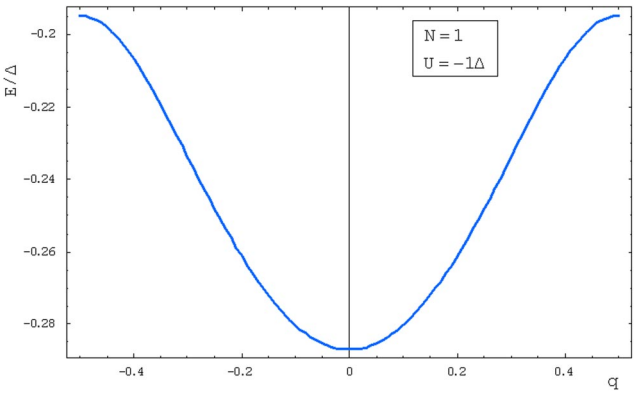

FIG. 10. (Color online) Bound state energy for a fixed attractive interaction as a function of the dimensionless crystal momentum q in the first Brillouin zone.

$$\frac{U}{\Delta} < \frac{N}{\sinh[\pi N]}(\cos[2\pi q] - \cosh[\pi N]), \tag{6.22}$$

the corresponding part of the band lies at negative energies (Fig. 6 provides such an example, with only a part of the band being negative).

The corresponding analysis for excited states ($B>0$) presents some interesting features, not present in the ground state energy behavior, which we briefly discuss in the following. We should emphasize in advance that these features can be directly linked to experimental results (hence providing a means of actually detecting the symmetry breaking) and, although they come up naturally in the context of the band-theoretic formulation advanced here, they are also present in ordinary ($\vartheta=0$) cases [provided that the various parameters are connected in the appropriate way, namely $q=-(f+N/2)$].

The key observation for the $B>0$ cases is that the lhs of the energy spectrum condition (6.15), which due to (6.18) can be written in a more suggestive form, namely

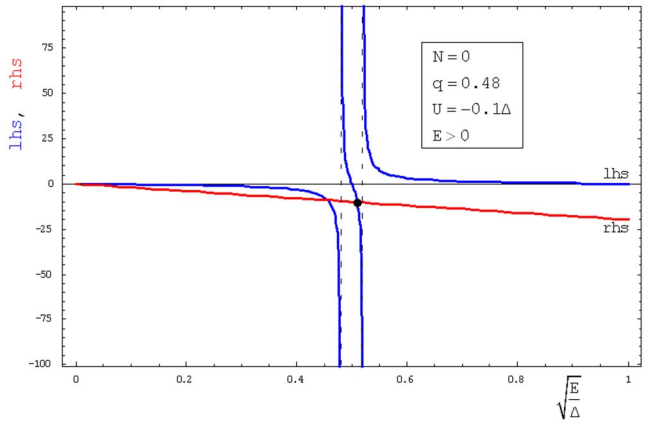

FIG. 11. (Color online) An example of a graphical solution of (6.23) with two very close divergences (when q is very close to the band edge $q=1/2$).

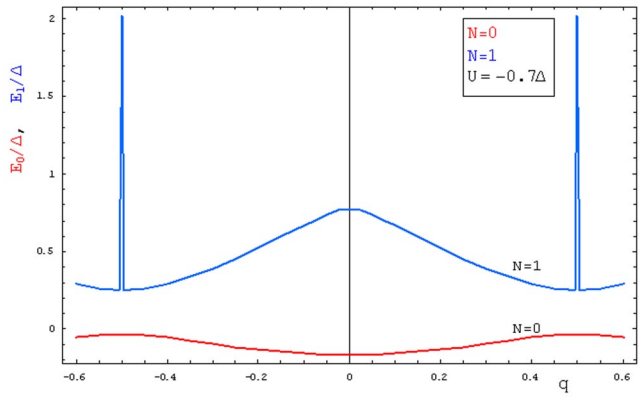

FIG. 12. (Color online) First excited state energy band with discontinuities at the ends of the zone (upper curve), shown together with the ground state band (lower curve) to emphasize energy differences.

$$\frac{\sin[2\pi\sqrt{B}]}{\cos[2\pi q]-\cos[2\pi\sqrt{B}]}=\frac{2\Delta\sqrt{B}}{U}, \tag{6.23}$$

has points of divergence at $\sqrt{B}=\pm q+\rho$ (ρ integer, playing the role of a reciprocal lattice vector) provided of course that $\sqrt{B}>0$. Consequently, when the parameters N, f, and ϑ are such that q is [through (6.18)] located exactly at the band edges (i.e., $q=\pm 1/2$) then, because of ρ, we have two divergences on top of each other (Fig. 5 actually providing such an example of double divergence for an ordinary case): if indeed q is moved infinitesimally (i.e., $q=-1/2+\varepsilon$, $\varepsilon>0$) then there appear two divergences, placed infinitesimally close to each other (i.e., at $\sqrt{B}=1/2+\varepsilon$ and $1/2-\varepsilon$); one diverges at positive and the other at negative infinity and the lhs of (6.23) connects the two infinities with a necessarily smooth way, hence with a rapidly decreasing curve that passes through zero (see Fig. 11). As a result, there always exists an intersection with the rhs of (6.23) which gives an allowed energy. However, this is *not* the case when q is *exactly* $\pm 1/2$: the two divergences are now "merged" into a double one, and at this point (6.23) does *not* have an allowed solution for B. Whenever this merging happens, a solution is "lost" (and is recovered whenever q moves slightly from the band edge). (An example was earlier shown in Fig. 5 of Sec. IV, where, because of this merging of divergences, there is not any intersection of rhs with the vertical dashed line). An important consequence of this peculiarity is that the "lost" solutions cause discontinuous raising of the allowed values of B whenever we are *exactly* at the band ends, since a solution of (6.23) (hence an intersection with its rhs) can only be found if we move to the next branch of the lhs. Figure 12 (upper curve) shows an example of such a discontinuous structure for the first excited state: on top of an inverted band with a local maximum at $q=0$, there appear two specific discontinuous positive jumps at the two band ends. [It turns out that for the second excited band and all the higher ones, a similar discontinuity also appears at $q=0$ (a result of the same merging of two discontinuities.)] Such a discontinuous behavior is never present in the ground state band (essentially because of the presence of hyperbolic rather than trigonometric functions). Therefore, the discontinuous rise observed at $q=\pm 1/2$ for the excited band makes the energy *difference* between the first excited and the ground state energy always be larger at $q=\pm 1/2$ than it is for $q=0$, actually being larger by more than $N^2/4$ (for $N=\pm 1$, at least). This is apparent in Fig. 12 where both bands are shown together, and it can have interesting consequences in exciton spectra (where transitions between the bands are involved): if we compare two cases of different N, i.e., $N=0$ and $N=-1$ (a chiral state, with a nonvanishing total angular momentum) in an experiment with a fixed f, then the above ordering of energy differences might have consequences on the position of peaks of exciton absorption or photoluminescence spectra (the simplest case being for ordinary state and $f=1/2$, when $N=0$ corresponds to the band edge and hence to a higher energy difference compared to the chiral state).

Let us finally see the effect of symmetry breaking on the modulus of the relative wave functions and on the other physical quantities, such as (6.6)–(6.9). First a straightforward determination of the relative normalization constant [$C=\Phi(0)$] for a general θ can be made [by using (6.14)] with the result

$$|C|^2=\frac{\sqrt{B}\,\sin^2[2\pi\sqrt{B}]}{\pi(4\pi\sqrt{B}-4\pi\sqrt{B}\,\cos[2\pi\sqrt{B}]\cos[2\pi f+N\pi-\vartheta]-\sin[4\pi\sqrt{B}]+2\,\sin[2\pi\sqrt{B}]\cos[2\pi f+\pi N-\vartheta])}$$

and direct substitution of a normalized relative wave function in (C1) results in a simple form for the probability density, namely

$$\rho(\overline{\varphi}) = \frac{1}{\pi R}, \tag{6.24}$$

a constant density that is simply equal to the expected $2/2\pi R$ for two particles moving in a length of $2\pi R$. This should actually be expected from the general form (C1) whenever the center of mass has a well-defined angular momentum $\hbar N$. The analogous calculation of the local charge density $\rho_{\mathrm{el}}(\overline{\varphi})$ gives, again for a fixed N,

$$\rho_{\mathrm{el}}(\overline{\varphi}) = 0. \tag{6.25}$$

The corresponding calculation for the remaining two quantities is rather tedious [i.e., they require use of (C3)] but it can be made analytically with the following results:

$$J(\overline{\varphi}) = \frac{\hbar\left(\frac{N}{R}\right)}{2m}\rho(\overline{\varphi}) = \frac{\hbar N}{2m\pi R^2}, \tag{6.26}$$

because the internal parts in (C3) are cancelled and only the center of mass contribution survives.

It should be noted that, although $|\Phi(\varphi)|$ *is* affected by the symmetry-breaking parameter θ, at the end $\rho(\overline{\varphi})$, $\rho_{\mathrm{el}}(\overline{\varphi})$, and $J(\overline{\varphi})$ are independent of θ, a result stronger than their required single-valuedness. On the contrary, for $J_{\mathrm{el}}(\overline{\varphi})$, which turns out to be

$$\begin{aligned} J_{\mathrm{el}}(\overline{\varphi}) = {} & \frac{i\hbar e}{4mR^2}\int_{\overline{\varphi}-2\pi}^{\overline{\varphi}} d\varphi |\Phi(\varphi)|^2 \left[\Psi_c\left(\overline{\varphi}-\frac{\varphi}{2}\right)\frac{\partial \Psi_c^*\left(\overline{\varphi}-\frac{\varphi}{2}\right)}{\partial\left(\overline{\varphi}-\frac{\varphi}{2}\right)} - \Psi_c^*\left(\overline{\varphi}-\frac{\varphi}{2}\right)\frac{\partial \Psi_c\left(\overline{\varphi}-\frac{\varphi}{2}\right)}{\partial\left(\overline{\varphi}-\frac{\varphi}{2}\right)} \right] \\ & + \frac{i\hbar e}{2mR^2}\int_{\overline{\varphi}-2\pi}^{\overline{\varphi}} d\varphi \left|\Psi_c\left(\overline{\varphi}-\frac{\varphi}{2}\right)\right|^2 \left[\Phi(\varphi)\frac{\partial\Phi^*(\varphi)}{\partial\varphi} - \Phi^*(\varphi)\frac{\partial\Phi(\varphi)}{\partial\varphi}\right] + \frac{i\hbar e}{2mR^2}\int_{-\overline{\varphi}}^{2\pi-\overline{\varphi}} d\varphi \left|\Psi_c\left(\overline{\varphi}+\frac{\varphi}{2}\right)\right|^2 \left[\Phi(\varphi)\frac{\partial\Phi^*(\varphi)}{\partial\varphi}\right. \\ & \left. - \Phi^*(\varphi)\frac{\partial\Phi(\varphi)}{\partial\varphi}\right] - \frac{i\hbar e}{4mR^2}\int_{-\overline{\varphi}}^{2\pi-\overline{\varphi}} d\varphi |\Phi(\varphi)|^2 \left[\Psi_c\left(\overline{\varphi}+\frac{\varphi}{2}\right)\frac{\partial \Psi_c^*\left(\overline{\varphi}+\frac{\varphi}{2}\right)}{\partial\left(\overline{\varphi}+\frac{\varphi}{2}\right)} - \Psi_c^*\left(\overline{\varphi}+\frac{\varphi}{2}\right)\frac{\partial \Psi_c\left(\overline{\varphi}+\frac{\varphi}{2}\right)}{\partial\left(\overline{\varphi}+\frac{\varphi}{2}\right)} \right] - \frac{e\hbar}{mR}\frac{\Phi}{\Phi_0}\rho(\overline{\varphi}), \end{aligned} \tag{6.27}$$

the opposite signs of the last two integrals compared to (C3) make the center of mass contributions essentially vanish and the internal (relative) part to give a nontrivial result. After straightforward manipulations this turns out to be

$$J_{\mathrm{el}}(\overline{\varphi}) = -\frac{4\pi e\sqrt{B}|C|^2\sin[2\pi f + \pi N - \vartheta]}{mR^2\sin[2\pi\sqrt{B}]}$$

or, alternatively,

$$J_{\mathrm{el}}(\overline{\varphi}) = -\frac{4e\Delta^2(\sqrt{B})^3\sin[2\pi f + \pi N - \vartheta]}{\hbar\{\sin[2\pi\sqrt{B}](4\pi\Delta B + U) - 2\pi U\sqrt{B}\cos[2\pi\sqrt{B}]\}}, \tag{6.28}$$

showing a direct dependence of the electric current on symmetry breaking.

We note that J_{el} is a nontrivial function of the various parameters and it depends on U through the appropriate solution of (6.15) for B. We also note from (6.18) that $J_{\mathrm{el}}(\overline{\varphi}) \propto \sin[2\pi q]$, and that, therefore, for a choice of ϑ corresponding to the center $q=0$ or the edge $q=\pm 1/2$ of the relative bands, we have $J_{\mathrm{el}}(\overline{\varphi})=0$. The electric current is here identical to the persistent currents as we demonstrate in the next section.

VII. PERSISTENT CURRENTS

The persistent currents I_n, usually defined (at $T=0$) for single-particle states with energy E_n as $I_n=-c(\partial E_n/\partial\Phi)$ with Φ the magnetic flux, are here determined in a similar manner but with use of the total energy E of the interacting two-particle system (when this is in a particular eigenstate), namely

$$I_{\mathrm{pers}} = -c\frac{\partial E}{\partial\Phi}, \tag{7.1}$$

where for notational simplicity we omit two indices that specify the eigenstate, namely N and one more index identifying the particular intersection point in the graphical solution of (6.15). For the particular system (where $A=\Phi/2\pi R$) we have $I_{\mathrm{pers}}=-(c/2\pi R)(\partial E/\partial A)$, but $\partial E/\partial A$ can be very generally determined through the use of the Hellmann-Feynman theorem with A being treated as a parameter: following earlier work[19,20] we have

$$\frac{\partial E}{\partial A} = \frac{\partial}{\partial A}\langle\Psi|\hat{H}|\Psi\rangle = \langle\Psi|\frac{\partial \hat{H}}{\partial A}|\Psi\rangle, \tag{7.2}$$

a statement equivalent to having $\langle\Psi|\Psi\rangle$: constant (independent of A). On the other hand, by making use of the system Hamiltonian

$$\hat{H} = \frac{1}{2m}\sum_{i=1}^{2}\left(p_i - \frac{q_i}{c}A\right)^2 \tag{7.3}$$

we easily obtain for (7.2) that

$$\frac{\partial E}{\partial A} = -\frac{2\pi R}{c}\langle J_{\rm el}\rangle \tag{7.4}$$

with the average (global) electric current being defined by

$$\langle J_{\rm el}\rangle = \frac{1}{2\pi R}\langle\Psi|\sum_{i=1}^{2}\frac{q_i}{m}\left(p_i - \frac{q_i}{c}A\right)|\Psi\rangle. \tag{7.5}$$

Equation (7.1) then rigorously leads to

$$I_{\rm pers} = \langle J_{\rm el}\rangle. \tag{7.6}$$

On the other hand, the *local* electric current density $J_{\rm el}(\overline{\varphi})$ [such as (6.28)] is the expectation value of the operator (6.4) and it directly gives the global current $\langle J_{\rm el}\rangle$ if integrated for all $\overline{\varphi}$, namely

$$\int_0^{2\pi} J_{\rm el}(\overline{\varphi})Rd\overline{\varphi} = 2\pi R\langle J_{\rm el}\rangle, \tag{7.7}$$

which through (7.6) gives the general connection between the local electric current and the persistent current, namely

$$I_{\rm pers} = \frac{1}{2\pi}\int_0^{2\pi} J_{\rm el}(\overline{\varphi})d\overline{\varphi}. \tag{7.8}$$

In the case of (6.28) $J_{\rm el}$ turns out to be homogeneous (independent of $\overline{\varphi}$), leading therefore to the expectation that, very generally (for a particular two-particle eigenstate) we have

$$J_{\rm el} = I_{\rm pers}, \tag{7.9}$$

an identification that should be expected on general physical grounds. To check that this equality actually holds in our case, it is possible to independently determine $I_{\rm pers}$ through (7.1) by differentiating the energy spectrum condition (6.15) with respect to Φ. Although tedious, it is straightforward, and this gives that $I_{\rm pers}$ is

$$I_{\rm pers} = -\frac{4e\Delta^2(\sqrt{B})^3\sin[2\pi f - \pi n - \vartheta]}{\hbar\{\sin[2\pi\sqrt{B}](4\pi\Delta B + U) - 2\pi U\sqrt{B}\cos[2\pi\sqrt{B}]\}}, \tag{7.10}$$

which is exactly equal to (6.28) (since N and n are of the same type), hence satisfying the expected (7.9). These results are valid for arbitrary symmetry breaking. In the limiting case that $U\to 0$ it is possible to show that (7.10) yields

$$I_{\rm pers}(U\to 0) = -\frac{e\hbar}{\pi mR^2}\left(f - \frac{n}{2} - \frac{\vartheta}{2\pi}\right), \tag{7.11}$$

which is the expected result for noninteracting particles (with $\vartheta = 0$ for ordinary states), in which case the total energy is simply

$$E(U\to 0) = \frac{\hbar^2 N^2}{4mR^2} + \frac{\hbar^2}{mR^2}\left(f - \frac{n}{2} - \frac{\vartheta}{2\pi}\right)^2 \tag{7.12}$$

and n can always be written as $n = n_1 - n_2$ ($n_{\rm i}$ integers), (7.11) simply indicating that the current results from the opposite contributions of separate single-particle currents. It should, however, be kept in mind that there is a periodicity of these results if written in terms of the "relative crystal momentum" q of the last section, with period 1 (see below). Furthermore, it is interesting to see how the persistent current is affected by the interaction in the limit of strong $|U|$, which is equivalent to the large radius limit and results such as (4.14) could be used in (7.1); for the ground state $I_{\rm pers}$ turns out to be exponentially small and it is equal to

$$I_{\rm pers} = \frac{eU^2}{\hbar\Delta}e^{-\pi(|U|/\Delta)}\sin[2\pi q]. \tag{7.13}$$

It should be noted that in this strong coupling limit all the excited state energies can also be given in closed form from which the associated persistent currents can also be found [through (7.1)], a matter that we will not pursue analytically any further. However, typical behaviors of $I_{\rm pers}$ with respect to the flux and the size of the ring will be shown in the figures at the end of the section.

It is more interesting to discuss briefly the general form of persistent currents (7.10) for an arbitrary interaction strength U. By temporarily going back to noninteracting particles, we note that (7.11) can be written [with use of (6.18)] as

$$I_{\rm pers}(U\to 0) = \frac{e\hbar}{\pi mR^2}q \tag{7.14}$$

and the corresponding energy spectrum (7.12) can now be written in a compact form as merely

$$B(U\to 0) = q^2. \tag{7.15}$$

It should, however, be kept in mind that, because of the ring topology and the associated periodicity in q [which can vary within the first Brillouin zone, Eq. (3.2)], there is a periodicity of both (7.15) and (7.14) with respect to q with period 1. Restricting ourselves therefore to the zone (3.2) this can be explicitly demonstrated by writing

$$I_{\rm pers}(U\to 0) = \frac{e\hbar}{\pi mR^2}(q + \rho) \tag{7.16}$$

and correspondingly

$$B(U\to 0) = (q + \rho)^2 \tag{7.17}$$

with ρ an appropriate integer (of any sign) that brings q within the first zone. This is essentially equivalent to the points of divergence that we found earlier at $\sqrt{B} = \pm q + \rho$ [which are indeed the only allowed solutions of (6.15) in the limit $U\to 0$, as the rhs tends to vertical lines]. The above

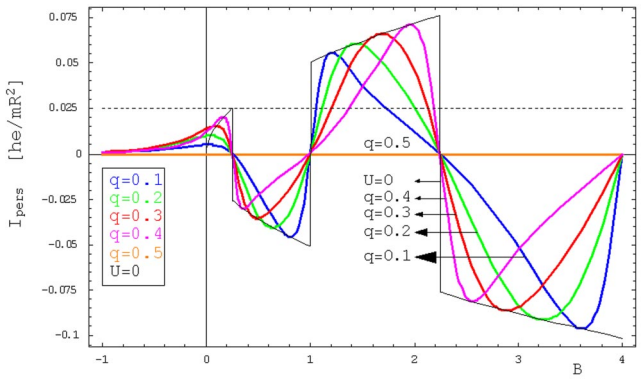

FIG. 13. (Color online) Persistent currents as a function of dimensionless internal energy (with interaction potential eliminated) for various values of q, demonstrating the comparison with the upper bound (7.18) (horizontal dashed line) and with the noninteracting ($U=0$) behavior (black curve).

presence of ρ is also equivalent to the expected periodicity when the relative integer n changes by multiples of 2 (i.e., by an even integer 2ρ), as this is the only change allowed for n to be of the same type as the center of mass integer N (N taken as fixed and given).

Having clarified this, it is easy to find the maximum value taken by $|I_{\text{pers}}|$ for the first zone and for $U=0$; this can be given by (7.14) with $|q|=\frac{1}{2}$. The result is

$$|I_{q=1/2}(U\to 0)| = \frac{he}{4\pi^2 mR^2}, \tag{7.18}$$

which is exactly the result found by Vignale[21] as a rigorous upper bound for persistent currents of any one-dimensional mesoscopic system of length L with $\bar{N}$ particles, namely

$$|I|_{\text{bound}} = \frac{\bar{N}he}{2mL^2}, \tag{7.19}$$

where in our case $\bar{N}=2$ and $L=2\pi R$. Having an equality for Vignale's bound for $U=0$, it is now interesting to let U have any arbitrary value and see whether (7.10) is generally smaller than (7.19). To check this, we first eliminate U from (7.10) with use of the energy spectrum condition (6.23) and in this way we obtain the general values of I_{pers} as a function of q [that contains f, N, and ϑ through (6.18)] and also of the allowed values of B (which are now forming a continuous set, and can be varied independently of q). We plot these values of I_{pers} in Fig. 13 for several values of q and we compare them with the upper bound (7.18) as well as with the noninteracting behavior (7.14) and (7.15). First, we note that, for $B>0$ the upper bound can be violated, but for $B<0$ we always have $|I_{\text{pers}}|<|I|_{\text{bound}}$. In fact, the ground state persistent currents seem to take their maximum absolute values whenever $B\to 0^-$, and this limit can be found analytically to be

$$|I_{\text{pers}}(B\to 0)| = \frac{3\Delta e}{2\pi^2\hbar}\left(\frac{\sin[2\pi q]}{2+\cos[2\pi q]}\right)$$
$$= \frac{3}{\pi}\left(\frac{\sin[2\pi q]}{2+\cos[2\pi q]}\right)|I|_{\text{bound}} \tag{7.20}$$

with a maximum value corresponding to $q=\frac{1}{3}$ and being

$$|I_{\text{pers}}(B<0)|_{\max} = \frac{\sqrt{3}}{\pi}|I|_{\text{bound}} \approx 0.551|I|_{\text{bound}}, \tag{7.21}$$

hence demonstrating the validity of the expected upper bound in the particular interacting system. (It should be noted that although existence of this bound was proven[21] for a system of only a single charged component, it seems to be also valid for our mixture of different charged components, and this could be shown in a more general setting in future work.) The qualitative reason why the inclusion of interactions leads to a lowering of $|I_{\text{pers}}|$ in the first zone with respect to the noninteracting case is the fact that $U\neq 0$ leads to the opening of gaps at the ends of the zone that were not present in the so-called empty lattice approximation ($U=0$). In Fig. 13 the current for the noninteracting case is also shown for comparison and provides a better understanding of the general interacting behavior. The combination of (7.14) with (7.15) yields a $\sqrt{B}$ behavior (black curve) which, however, changes sign whenever B corresponds to values of q that move to higher zones: the procedure of reduction to the first zone effectively changes the sign of q and, through (7.14), of the noninteracting current itself. The general interacting behavior demonstrates more interesting oscillatory variations with B but it qualitatively follows a similar pattern of sign changes, as expected. A feature of the interacting behavior (that is naturally absent in the $U=0$ case) is the presence of a $B<0$ tail (cases of binding), this now being monotonic (nonoscillatory). A final comment on Fig. 13 refers to the exact vanishing of I_{pers} at special points $B=(\text{integer}/2)^2$ (with a nonzero integer) for all possible q. These are related to the case $|U|\to\infty$, in which all bands become flat (zero bandwidth), hence with vanishing current for all q, the flat ground state band's contribution to the energy (for $B<0$) having moved to $-\infty$, as is apparent from the left part of Fig. 13.

The behavior of the persistent current (with interactions included) with combined variations of q (essentially the flux) and B (essentially the energy), for excited states ($B>0$) and after elimination of U, is shown in Fig. 14 for a typical size of a GaAs/AlGaAs nanoring. Figures 15 and 16 show examples of typical behavior for such a system as a function of flux (recall that $q=-f-N/2+\vartheta/2\pi$). Figure 15 focuses on a fixed attractive interaction (and varying energies), while Fig. 16 focuses on fixed energies [and elimination of U through (6.23)]. Both cases of positive and negative values of B are shown and the noninteracting (linear in q) behavior is also superimposed for comparison. Several observations can be made but we only mention the tangential behavior of the $U=0$-line on the interacting curve for certain positive values of B, but also cases (again for $B>0$) where $|I_{\text{pers}}|$ exceeds the magnitude of the noninteracting current. When $B\to 0$, the

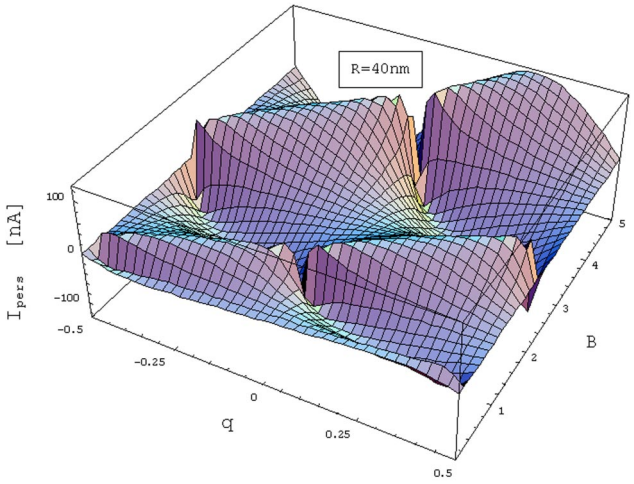

FIG. 14. (Color online) Behavior of persistent currents (with interaction eliminated) for a GaAs/AlGaAs nanoring of a typical size with respect to combined variations of energy and flux (recall $B=E/\Delta-N^2/4$ and $q=-f-N/2+\vartheta/2\pi$).

behavior approaches the noninteracting line. Finally, Figs. 17–20 present typical behaviors of persistent currents with respect to the size of the ring. Figures 17 and 18 focus on fixed attractive interactions, while Figs. 19 and 20 show cases with fixed energies (and with U being eliminated). We note that, for cases of binding $(B<0)$, $|I_{\text{pers}}|$ is always smaller than the magnitude of the noninteracting current, and it very quickly approaches zero above some values of the radius close to the typical ones in experiments with GaAs/AlGaAs nanorings (Fig. 18). On the contrary, for $B>0$, we note an interesting crossover around $R\sim 20$ nm (Fig. 17); for rings with radius smaller than this value, the attractive interaction seems to enhance conduction compared to the noninteracting case. (It is interesting that a similar crossover does *not* appear for a repulsive U, and $|I_{\text{pers}}|$ is always smaller than the noninteracting value). Cases of fixed positive energy (with U eliminated) present some additional oscillatory structure, and examples are shown in Figs. 19 and 20 (where because of different N's, both cases correspond to the same value of flux, namely $f=-0.1$, if we constraint ourselves to ordinary states $\vartheta=0$). We note different behaviors for very small rings depending on chirality, as well as several crossovers where $|I_{\text{pers}}|$ again exceeds the magnitude of the noninteracting current. It should be added that such crossovers do *not* appear in cases of binding (i.e., a fixed negative B) where $|I_{\text{pers}}|$ is monotonic and always smaller than the noninteracting value.

The exact form of the persistent currents that we have at our disposal for this particular interacting mixture leads us to a final observation that seems, however, to have a more general validity and is presented in the following section.[22]

VIII. BERRY'S PHASE

Since electron or hole systems in a nanoring have recently raised considerable interest in the area of quantum computation, and in particular the use of geometric (rather than dynamic) phases is currently considered in possible design of quantum gates,[23] we are now presenting some exact properties that relate the electric (persistent) currents of our system with the Berry's phase of some particular cyclic adiabatic process, to be defined below. It should be reemphasized that cyclic adiabatic evolution can find useful application in fault tolerant quantum computation, and we consider it important to have a direct connection between corresponding Berry's phases and concrete (and controllable) physical quantities, such as the electric current.

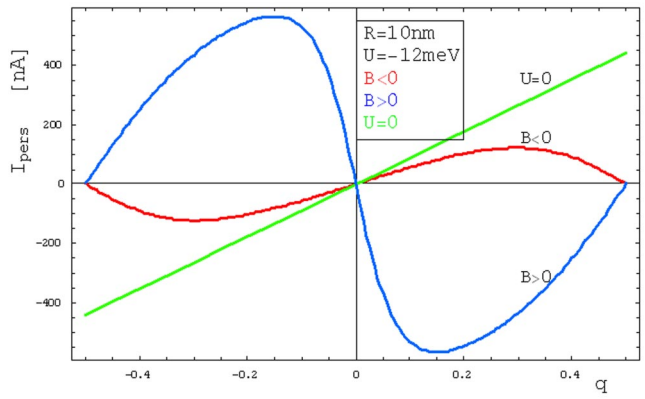

FIG. 15. (Color online) Persistent currents vs q for fixed attractive interaction and for both signs of internal energy (which is not fixed but varies along the curves) and a comparison with the noninteracting behavior.

Let us initially generalize the form of our interparticle interaction to $U\delta(\varphi_1-\varphi_2-\varphi_0)$ with φ_0 a real angular parameter that is supposed to move adiabatically in the region $[0,2\pi]$. This means that $0\leqslant\varphi_0(t)\leqslant 2\pi$ with $\varphi_0(t)$ changing in such a way that at every instant the rate $\dot{\varphi}_0(t)$ satisfies $\hbar\dot{\varphi}_0(t)\ll$ (absolute value of the lowest energy difference between states of our system). We find that such a simple adiabatic criterion is $\hbar\dot{\varphi}_0(t)\ll\Delta/4$ (corresponding to transitions $N\to N\pm 1$). Such a slow variation of φ_0 along a full circle takes the Hamiltonian of the system back to its initial form; the eigenstates however (the ones that were analytically determined in this work) will pick up an additional phase, of a

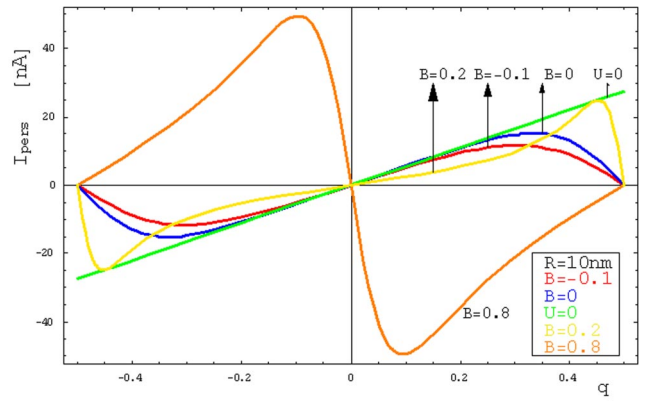

FIG. 16. (Color online) Persistent currents vs q for fixed internal energies of both signs (with interaction being eliminated) and comparison with the noninteracting behavior.

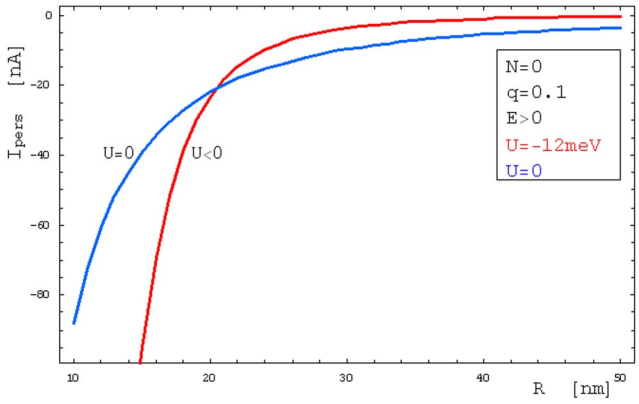

FIG. 17. (Color online) Persistent currents vs ring radius for fixed attractive interaction and for positive energies (which vary along the curves) showing a crossover with noninteracting behavior.

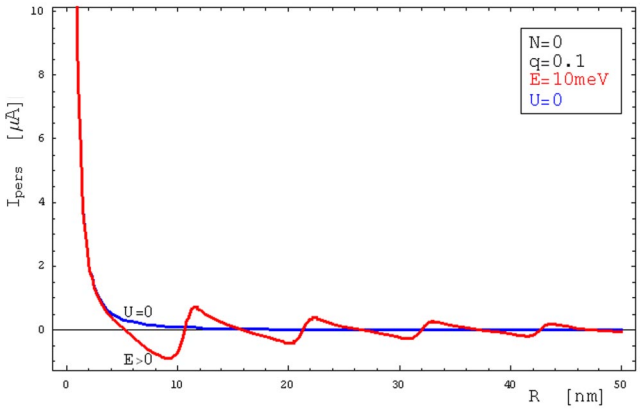

FIG. 19. (Color online) Persistent currents vs ring radius for fixed positive energy (and U eliminated) showing a series of crossovers with noninteracting behavior.

purely geometric nature, that was found by Berry[14] to be

$$\gamma_n = i \oint d\varphi_0 \left\langle n(\varphi_0) \left| \frac{\partial n(\varphi_0)}{\partial \varphi_0} \right. \right\rangle, \tag{8.1}$$

where the symbol n now denotes collectively the particular eigenstate considered.

With use of a resolution of the identity operator in relative and center of mass variables, (8.1) can be written as

$$\gamma_n = i \int_{-2\pi}^{2\pi} d\varphi \int_0^{2\pi} d\Phi_c \int_0^{2\pi} d\varphi_0 \Psi^*_{\varphi_0}(\varphi, \Phi_c) \frac{\partial \Psi_{\varphi_0}(\varphi, \Phi_c)}{\partial \varphi_0}, \tag{8.2}$$

where Ψ_{φ_0} denotes the total eigenfunction (for each instantaneous value of the adiabatic parameter φ_0) which in variables φ, Φ_c is simply a product, namely

$$\Psi_{\varphi_0}(\varphi, \Phi_c) = \Psi_c(\Phi_c)\Phi(\varphi - \varphi_0). \tag{8.3}$$

In (8.3) $\Psi_c(\Phi_c)$ is basically given by (2.6) and is independent of φ_0, and $\Phi(\varphi - \varphi_0)$ is given by (5.1) [or (6.14) if we allow for symmetry breaking] but with variable φ simply substituted by $\varphi - \varphi_0$. Use of all this in (8.2) gives, after rather tedious but straightforward manipulations, the Berry's phase picked up by the total eigenstate during this cyclic process, the result being

$$\gamma_n = 2\pi \frac{\Phi}{\Phi_0} - \frac{\pi h}{\Delta e} \frac{4e\Delta^2(\sqrt{B})^3 \sin[2\pi f - \pi n - \vartheta]}{\hbar(\sin[2\pi\sqrt{B}](4\pi\Delta B + U) - 2\pi U\sqrt{B}\cos[2\pi\sqrt{B}])}. \tag{8.4}$$

Direct comparison with (7.10) leads to an exact property (for any symmetry-breaking parameter ϑ), namely

$$\gamma_n = 2\pi \frac{\Phi}{\Phi_0} + \frac{\pi h}{\Delta e} J_{\text{el}}. \tag{8.5}$$

The first term is recognized as the Aharonov-Bohm contribution, i.e., the one found by Berry for the adiabatic transport of a bound state (in a box with rigid walls) around the enclosed magnetic flux $\Phi = f\Phi_0$. The second term is a contribution due to the extended coherent nature of the eigenstates

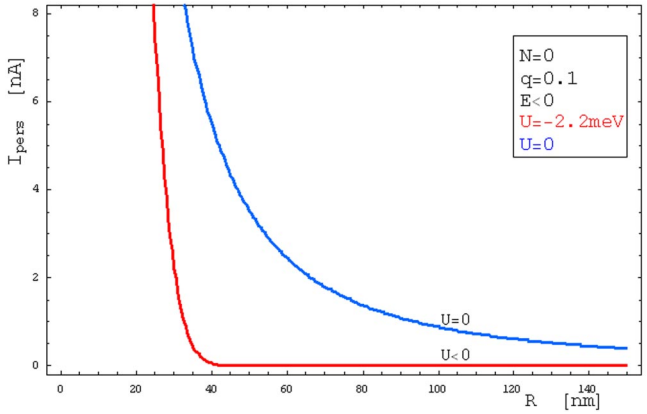

FIG. 18. (Color online) Persistent currents vs ring radius for fixed attractive interaction and for cases of binding, compared to the noninteracting behavior.

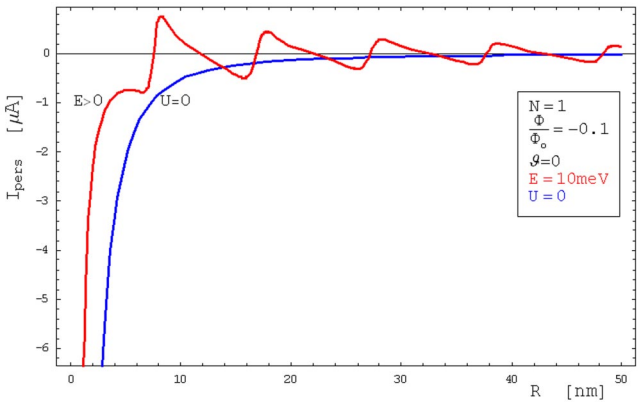

FIG. 20. (Color online) Similar to Fig. 19 (if we are constrained to ordinary states, both cases correspond to the same value of f) but for a chiral state.

around the ring, and it is found here to be directly linked to the electric (persistent) current [and *not* the probability current (6.26)] determined for $\varphi_0=0$ (although the value of $J_{\rm el}$ is actually independent of φ_0, as will be shown below).

Let us now briefly investigate the generality or possible extensions of (8.5). An initial plausible question is whether (8.5) could also be valid for a more general form of interparticle interaction $U(\varphi_1-\varphi_2)$, even in cases when the problem might be impossible to solve exactly. The answer seems to be positive and makes full use of the operator forms (6.1)–(6.4); but before we demonstrate this, let us first digress and discuss the corresponding one-particle problem. This is not entirely equivalent to our charged mixture, as we will see (since electric and probability currents now differ only by a global charge factor), but it will set a large part of the logic that needs to be followed.

We first consider, therefore, a single particle (of charge q and mass m) moving along a ring of circumference $L=2\pi R$ (or, equivalently, in a region of size L in straight one-dimensional space, with periodic boundary conditions imposed) and under the action of a potential $U(x-x_0)$ with $x_0(t)$ denoting the slowly varying parameter, but otherwise the form of U being arbitrary.

The average (global) electric current when the system is in state $\Psi(x)$ [essentially (7.5)] is

$$\langle J_{\rm el}\rangle = \frac{i\hbar q}{2mL}\int dx\left[\Psi(x)\frac{\partial\Psi^*(x)}{\partial x}-\Psi^*(x)\frac{\partial\Psi(x)}{\partial x}\right] - \frac{q^2}{mcL}\int dx\, A(x)|\Psi(x)|^2, \tag{8.6}$$

where integrations are along the region L (or around the ring). This can be further simplified into

$$\langle J_{\rm el}\rangle = -\frac{i\hbar q}{mL}\int dx\Psi^*(x)\frac{\partial\Psi(x)}{\partial x}-\frac{q^2}{mcL}\int dx\, A(x)|\Psi(x)|^2, \tag{8.7}$$

as is easily seen with integration by parts and the vanishing of $|\Psi(x)|^2$ at the end points (single-valuedness of $|\Psi|^2$). Equivalently, one could use the requirement of reality of momentum $\langle\Psi|\hat{p}|\Psi\rangle$ (as the momentum operator is self-adjoint in a ring), that also leads to

$$\int dx\Psi(x)\frac{\partial\Psi^*(x)}{\partial x}=-\int dx\Psi^*(x)\frac{\partial\Psi(x)}{\partial x}. \tag{8.8}$$

(We place emphasis on this, since a similar argument of self-adjointness will also be used below for kinetic energy leading to interesting consequences.) Now a key observation can be made about any eigenfunction $\Psi(x)$: since the natural variable is $(x-x_0)$ (position measured with respect to the potential center), we expect that eigenfunctions will depend on parameter x_0 only in the form $\Psi(x-x_0)$, a statement equivalent to the fact that any normalization constant will be independent of x_0, namely

$$\frac{\partial\langle\Psi|\Psi\rangle}{\partial x_0}=0. \tag{8.9}$$

Consequently, we can always make the following important substitution:

$$\frac{\partial\Psi(x-x_0)}{\partial x}=-\frac{\partial\Psi(x-x_0)}{\partial x_0} \tag{8.10}$$

which if used in (8.7) leads to

$$\langle J_{\rm el}\rangle = \frac{i\hbar q}{mL}\int dx\Psi^*(x)\frac{\partial\Psi(x)}{\partial x_0}-\frac{q^2}{mcL}\int dx\, A(x)|\Psi(x)|^2. \tag{8.11}$$

(It should be noted that use of (8.10) in (8.8) simply leads to (8.9), showing the self-consistency of the argument). Equation (8.11) gives the global current for any instantaneous value of x_0.

On the other hand, after x_0 is adiabatically moved around the circle $[0\leqslant x_0(t)\leqslant 2\pi]$, the Berry's phase picked up by any eigenstate (labeled by index n) is

$$\gamma_n = i\oint dx_0\left\langle\Psi\left|\frac{\partial\Psi}{\partial x_0}\right.\right\rangle = i\int_0^{2\pi}dx_0\int_0^{2\pi}dx\;\Psi^*(x)\frac{\partial\Psi(x)}{\partial x_0}. \tag{8.12}$$

Comparison of (8.11) and (8.12) immediately gives

$$\gamma_n=\frac{mL}{\hbar q}\oint dx_0\langle J_{\rm el}\rangle+\frac{q}{\hbar c}\oint dx_0\langle A(x)\rangle, \tag{8.13}$$

which is a first important result. This can be simplified further if we make the choice $|A(x)|=\Phi/2\pi R$ (with Φ some Aharonov-Bohm flux threading the ring) and if we note that $\langle J_{\rm el}\rangle$ is expected to be independent of the instantaneous value of x_0. This is true because direct evaluation of $(\partial/\partial x_0)\langle J_{\rm el}\rangle$, in combination with (8.10) and after integration by parts, yields

$$\frac{\partial}{\partial x_0}\langle J_{\rm el}\rangle=-\frac{i\hbar q}{2mL}\int dx\left(\Psi(x)\frac{\partial^2\Psi^*(x)}{\partial x^2}-\Psi^*(x)\frac{\partial^2\Psi(x)}{\partial x^2}\right), \tag{8.14}$$

which is zero due to the expected reality of kinetic energy (or the self-adjointness of operator $\hat{p}^2$).

The independence of $\langle J_{\rm el}\rangle$ of x_0 turns (8.13) into

$$\gamma_n=\frac{2\pi h}{q\Delta}\langle J_{\rm el}\rangle+2\pi\frac{q}{e}\frac{\Phi}{\Phi_0} \tag{8.15}$$

with $\Delta=\hbar^2/mR^2$, a result that is the analog of (8.5), the factor of 2 difference being due to the single-particle system. It should be reemphasized that (8.15) is valid independent of the interaction potential. Before we return to our two-particle problem, we should note that properties such as (8.13) seem to be generalizable to higher dimensionality, to relations of the form (for a two-dimensional system of area S with $\vec{r}_0$ being the adiabatic parameter moving in a closed path)

$$\gamma_n = \frac{mS}{\hbar q}\oint d\vec{r}_0 \cdot \langle \vec{J}_{\rm el}\rangle + \frac{q}{\hbar c}\oint d\vec{r}_0 \cdot \langle \vec{A}(\vec{r})\rangle \qquad (8.16)$$

and this leads to interesting properties concerning two-dimensional quantal behavior in an external magnetic field.[22] Similar forms appear for the three-dimensional analog.

After this digression let us go back to our system of two particles but with an arbitrary interparticle interaction potential. We introduce again the angular adiabatic parameter $\varphi_0(t)$ in $U(\varphi_1-\varphi_2-\varphi_0(t))$ which is now varied in the "relative circle" $[0\leqslant\varphi_0(t)\leqslant 2\pi]$ and study the possible connection of the Berry's phase picked up by any eigenstate with some average current. We will here find that, for a neutral system, the connection involves only the electric current and has no relation to the probability current, although this conclusion will be generalized further to a non-neutral system at the end.

First, operator (6.4) with the choice $\vec{A}(\overline{\varphi})=(\Phi/2\pi R)\hat{\varphi}$ and use of (6.1) takes the form

$$\hat{J}_{\rm el}(\overline{\varphi}) = \frac{1}{2R}\sum_{i=1}^{2} q_i\left(\frac{\hat{p}_i}{m_i}\delta(\overline{\varphi}-\varphi_i) + \delta(\overline{\varphi}-\varphi_i)\frac{\hat{p}_i}{m_i}\right) - \frac{\hbar q^2}{meR}\frac{\Phi}{\Phi_0}\rho(\overline{\varphi}) \qquad (8.17)$$

with the understanding that it points to the $\hat{\varphi}$ direction, and for our system we set $q_1=-q_2=q$. Taking the expectation value of (8.17) with respect to any eigenstate of this two-particle system, but *without* carrying out the integration with respect to φ_1 or φ_2, leads to the local electric current

$$J_{\rm el}(\overline{\varphi}) = \frac{i\hbar}{2mR^2}\int d\varphi_1 d\varphi_2 \sum_{i=1}^{2} q_i \begin{pmatrix} \delta(\overline{\varphi}-\varphi_i)\Psi(\varphi_1,\varphi_2)\dfrac{\partial\Psi^*(\varphi_1,\varphi_2)}{\partial\varphi_i} \\ -\delta(\overline{\varphi}-\varphi_i)\Psi^*(\varphi_1,\varphi_2)\dfrac{\partial\Psi(\varphi_1,\varphi_2)}{\partial\varphi_i}\end{pmatrix} - \frac{\hbar q^2}{meR}\frac{\Phi}{\Phi_0}\rho(\overline{\varphi}). \qquad (8.18)$$

An eventual integration with respect to $\overline{\varphi}$ will lead to the average (global) electric current [see (7.7)], namely $\langle J_{\rm el}\rangle = (1/2\pi)\int_0^{2\pi} d\overline{\varphi} J_{\rm el}(\overline{\varphi})$; the integration will set all delta-functions to unity giving the result

$$\langle J_{\rm el}\rangle = \frac{i\hbar}{4\pi mR^2}\int d\varphi_1 d\varphi_2 \sum_{i=1}^{2} q_i\left(\Psi(\varphi_1,\varphi_2)\frac{\partial\Psi^*(\varphi_1,\varphi_2)}{\partial\varphi_i} - \Psi^*(\varphi_1,\varphi_2)\frac{\partial\Psi(\varphi_1,\varphi_2)}{\partial\varphi_i}\right) - \frac{\hbar q^2}{meR}\frac{\Phi}{\Phi_0}\langle\rho\rangle, \qquad (8.19)$$

where $\langle\rho\rangle=(1/2\pi)\int_0^{2\pi}d\overline{\varphi}\rho(\overline{\varphi})$, which is quite generally expected to be $\langle\rho\rangle=2/2\pi R$. By following then a similar line of approach as in the digression, we use

$$\int d\varphi_1 d\varphi_2 \Psi(\varphi_1,\varphi_2)\frac{\partial\Psi^*(\varphi_1,\varphi_2)}{\partial\varphi_i} = -\int d\varphi_1 d\varphi_2 \Psi^*(\varphi_1,\varphi_2)\frac{\partial\Psi(\varphi_1,\varphi_2)}{\partial\varphi_i} \qquad (8.20)$$

(essentially due to the single-valuedness of $|\Psi|^2$ with respect to each φ_i and an integration by parts) to bring (8.19) to the form

$$\langle J_{\rm el}\rangle = -\frac{i\hbar}{2\pi mR^2}\int d\varphi_1 d\varphi_2\left(q\Psi^*(\varphi_1,\varphi_2)\frac{\partial\Psi(\varphi_1,\varphi_2)}{\partial\varphi_1} - q\Psi^*(\varphi_1,\varphi_2)\frac{\partial\Psi(\varphi_1,\varphi_2)}{\partial\varphi_2}\right) - \frac{\hbar q^2}{meR}\frac{\Phi}{\Phi_0}\langle\rho\rangle. \qquad (8.21)$$

Now, the important step is to change to center of mass and relative variables (2.2), namely

$$\frac{\partial}{\partial\varphi_1} = \frac{1}{2}\frac{\partial}{\partial\Phi_c} + \frac{\partial}{\partial\varphi}, \quad \frac{\partial}{\partial\varphi_2} = \frac{1}{2}\frac{\partial}{\partial\Phi_c} - \frac{\partial}{\partial\varphi} \qquad (8.22)$$

which, for our neutral system, will cancel all derivatives in (8.21) with respect to Φ_c, leaving the form

$$\langle J_{\rm el}\rangle = -\frac{i\hbar q}{\pi mR^2}\int d\varphi\int d\Phi_c\left(\Psi^*(\varphi,\Phi_c)\frac{\partial\Psi(\varphi,\Phi_c)}{\partial\varphi}\right) - \frac{\hbar q^2}{meR}\frac{\Phi}{\Phi_0}\langle\rho\rangle. \qquad (8.23)$$

If we finally consider the adiabatic motion of parameter φ_0, the dependence (in the new variables) of the potential is $U(\varphi-\varphi_0)$ and of the two-particle wave functions is $\Psi(\varphi-\varphi_0,\Phi_c)$, which allows the important substitution

$$\frac{\partial\Psi(\varphi-\varphi_0,\Phi_c)}{\partial\varphi} = -\frac{\partial\Psi(\varphi-\varphi_0,\Phi_c)}{\partial\varphi_0} \qquad (8.24)$$

to yield

$$\langle J_{\rm el}\rangle = \frac{i\hbar q}{\pi mR^2}\int_{-2\pi}^{2\pi} d\varphi\int_0^{2\pi} d\Phi_c\left(\Psi^*(\varphi,\Phi_c)\frac{\partial\Psi(\varphi,\Phi_c)}{\partial\varphi_0}\right) - \frac{\hbar q^2}{meR}\frac{\Phi}{\Phi_0}\langle\rho\rangle, \qquad (8.25)$$

a result that gives the global electric current for any instantaneous value of φ_0. On the other hand, after φ_0 is varied around the relative circle, the Berry's phase picked up by the two-particle wave function (denoted again by symbol n) will be

$$\gamma_n = i\int_0^{2\pi} d\varphi_0 \int_{-2\pi}^{2\pi} d\varphi \int_0^{2\pi} d\Phi_c \Psi^*(\varphi,\Phi_c)\frac{\partial \Psi(\varphi,\Phi_c)}{\partial \varphi_0} \tag{8.26}$$

and direct comparison with (8.25) leads to

$$\gamma_n = \frac{\pi m R^2}{\hbar q}\int d\varphi_0 \langle J_{\rm el}\rangle + \frac{q\pi R}{e}\frac{\Phi}{\Phi_0}\int d\varphi_0 \langle \rho\rangle. \tag{8.27}$$

This is a first important result that can be simplified further if we again note that $\langle J_{\rm el}\rangle$ is expected to be independent of φ_0. This can again be shown by direct evaluation of $(\partial/\partial\varphi_0)\langle J_{\rm el}\rangle$ that yields

$$\frac{\partial}{\partial \varphi_0}\langle J_{\rm el}\rangle = \frac{i\hbar q}{2\pi m R^2}\int d\varphi \int d\Phi_c \left(\Psi \frac{\partial^2 \Psi^*}{\partial \varphi^2} - \Psi^* \frac{\partial^2 \Psi}{\partial \varphi^2}\right), \tag{8.28}$$

which can be taken as zero since the relative kinetic energy is real. This independence of $\langle J_{\rm el}\rangle$ of φ_0 turns (8.27) into

$$\gamma_n = \frac{\pi h}{\Delta q}\langle J_{\rm el}\rangle + 2\pi \frac{q}{e}\frac{\Phi}{\Phi_0} \tag{8.29}$$

an exact general property in agreement with (8.5) that was earlier derived for our δ-function potential (with $q=e$). [To derive (8.29) we used that $\langle \rho\rangle = 2/2\pi R$.]

A better understanding of the above properties can be acquired if we briefly mention a generalization to an arbitrary mixture of charges q_1 and q_2. In such case, the probability current is also involved, as we finally demonstrate.

The analog of (8.21) is now

$$\langle J_{\rm el}\rangle = -\frac{i\hbar}{2\pi m R^2}\int d\varphi_1 \int d\varphi_2 \left(q_1 \Psi^*(\varphi_1,\varphi_2)\frac{\partial \Psi(\varphi_1,\varphi_2)}{\partial \varphi_1} + q_2 \Psi^*(\varphi_1,\varphi_2)\frac{\partial \Psi(\varphi_1,\varphi_2)}{\partial \varphi_2}\right) - \frac{\hbar(q_1^2+q_2^2)}{me\mathrm{R}}\frac{\Phi}{\Phi_0}\langle \rho\rangle, \tag{8.30}$$

which in new variables reads

$$\langle J_{\rm el}\rangle = -\frac{i\hbar(q_1+q_2)}{2\pi m R^2}\int d\varphi \int d\Phi_c \left(\Psi^*(\varphi,\Phi_c)\frac{\partial \Psi(\varphi,\Phi_c)}{\partial \Phi_c}\right) - \frac{i\hbar}{2\pi m R^2}(q_1-q_2)\int d\varphi \int d\Phi_c \Psi^*(\varphi,\Phi_c)\frac{\partial \Psi(\varphi,\Phi_c)}{\partial \varphi} - \frac{\hbar(q_1^2+q_2^2)}{me\mathrm{R}}\frac{\Phi}{\Phi_0}\langle \rho\rangle. \tag{8.31}$$

We note the extra appearance of the first term, which is actually related to the global probability current $\langle J\rangle$. Indeed, direct use of (6.3) and transformation to the new variables yields

$$\langle J\rangle = -\frac{i\hbar}{2\pi m R^2}\int d\varphi \int d\Phi_c \left(\Psi^*(\varphi,\Phi_c)\frac{\partial \Psi(\varphi,\Phi_c)}{\partial \Phi_c}\right) - \frac{\hbar(q_1+q_2)}{me\mathrm{R}}\frac{\Phi}{\Phi_0}\langle \rho\rangle \tag{8.32}$$

so that the first term of (8.31) can be immediately connected to $\langle J\rangle$.

The second term of (8.31) can then be connected with the Berry's phase (8.26) if the important substitution (8.24) is made. The final result of all this has the form

$$\gamma_n = \frac{2\pi m R^2}{\hbar(q_1-q_2)}\int_0^{2\pi} d\varphi_0 \langle J_{\rm el}\rangle - \frac{2\pi m R^2(q_1+q_2)}{\hbar(q_1-q_2)}\int_0^{2\pi} d\varphi_0 \langle J\rangle - \frac{2\pi R q_1 q_2}{e(q_1-q_2)}\frac{\Phi}{\Phi_0}\int_0^{2\pi} d\varphi_0 \langle \rho\rangle \tag{8.33}$$

provided, of course, that $q_1 \neq q_2$. In the special case $q_1=-q_2=q$, this recovers (8.27) for a neutral system.

Two major comments should be made on the above generalization. First, the probability current does not appear in any way if the system is neutral. Second, the case $q_1=q_2$ [not covered by (8.33)], which is actually the most common case of a single-component system (i.e., of identical particles) in many-body treatments of charged particles, does not lead to any connection of the Berry's phase with either $\langle J\rangle$ or $\langle J_{\rm el}\rangle$. The reason is that, for $q_1=q_2$, the second term of (8.31) is missing, the derivatives $\partial/\partial\varphi$ are therefore entirely absent [from both (8.31) and (8.32)] and the important property (8.24) does not have any role whatsoever, so that no connection can be made between either of the currents and the Berry's phase (8.26).

Although general relations such as (8.33), connecting geometric phases with controllable physical quantities, such as currents, could be useful in the design of qubits based on two-particle nanorings, a further generalization to arbitrary interacting mixtures of N particles would be important as a general constraint on many-body treatments of relevant systems.

IX. CONCLUSIONS

In the present work the simplest model problem of an interacting quantal charged mixture moving in a doubly connected space and in the presence of an Aharonov-Bohm flux was exactly solved, revealing some interesting properties that seem to have a higher generality. These properties, together with all other results derived in this paper, are exact and were determined in closed analytical forms. They might, therefore, be useful in advancing possible effective two-particle descriptions of more complicated many-body systems in Aharonov-Bohm settings.

The model problem consisted initially of a neutral system of two interacting charged particles moving in a one-dimensional ring, threaded by a magnetic flux, and with a contact interaction. The energy spectrum and the associated eigenstates were exactly determined and analytical criteria for transitions from excited to bound states were given and

compared with earlier literature on many-body interacting mixtures. A closer investigation of measurable quantities and their single-valuedness led to states with broken symmetry and to a new band-mode structure with possible experimental consequences in exciton physics. Probability and electric (persistent) currents were also analytically determined for this interacting quantal mixture and some of their interesting properties were revealed. In particular, the exact form of persistent currents enabled us to make an investigation of their behavior with respect to combined variations of several parameters such as the energy, interaction strength, size of the ring, magnetic flux, symmetry breaking parameter, and pair angular momentum. We compared these results with exact theorems on persistent currents, such as a rigorous upper bound known in the literature and also with the noninteracting behavior, where an interesting crossover was found for attractive interaction and sufficiently small rings. Finally, a cyclic adiabatic process on the interaction potential center was identified that led to a geometric (Berry's) phase directly linked to the electric (persistent) currents, with no relation to the probability currents for a neutral system. It was shown how these results can be generalized to systems of higher dimensionality, as well as to non-neutral mixtures, in which case the geometric phase is directly connected to both types of currents. The link to the probability current was shown always to appear only through the total charge of the system (and it disappears under conditions of neutrality). The link of the geometric phase to either current was shown not to appear for systems of a single charged component, the character of a mixture hence being crucial for the properties revealed in this work. Such properties may possibly find useful application not only to exciton physics but also to the field of fault tolerant quantum computation. Moreover, possible generalization to an arbitrary charged quantal mixture of any number of interacting components would be of obvious importance to many-body physics, and it is an issue that is currently under investigation.

APPENDIX A

We here present the mathematical details associated with the finding of $G(\varphi,\varphi')$ that solves (2.10) for $-\pi<\varphi,\varphi'\leqslant\pi$, under boundary conditions that are dictated by (3.7), namely

$$G(\pi,\varphi')=e^{i\theta}G(-\pi,\varphi'),$$
$$\frac{\partial}{\partial\varphi}G(\varphi,\varphi')\bigg|_{\varphi\to\pi}=e^{i\theta}\ \frac{\partial}{\partial\varphi}G(\varphi,\varphi')\bigg|_{\varphi\to-\pi}. \tag{A1}$$

Equation (2.10) can first be simplified by an initial transformation, namely $G(\varphi,\varphi')=e^{if\ \varphi}\tilde{G}(\varphi,\varphi')$, which brings it to a new and simpler equation for $\tilde{G}$, namely

$$\left(\frac{\partial^2}{\partial\varphi^2}+B\right)\tilde{G}(\varphi,\varphi')=\delta(\varphi-\varphi'). \tag{A2}$$

[This can either be viewed as a transformation to the normal form of (2.10) involving the Wronskian $e^{2if\varphi}$, or as the familiar Aharonov-Bohm phase factor $e^{if\varphi}$ that connects corresponding problems in a ring, with vanishing and nonvanishing magnetic flux.] Then, by following the usual matching procedure, we first choose an arbitrary φ' (within the interval $(-\pi,\pi]$) treating it as a constant, and solve (A2) for $\varphi\neq\varphi'$, as a homogeneous Helmholtz equation for $\tilde{G}(\varphi)$. Then, after we go back to the original Green's function we obtain

$$G_R(\varphi,\varphi')=ae^{i(f+\sqrt{B})\varphi}+be^{i(f-\sqrt{B})\varphi}\quad\text{for}\quad\varphi>\varphi' \tag{A3}$$

and

$$G_L(\varphi,\varphi')=ce^{i(f+\sqrt{B})\varphi}+de^{i(f-\sqrt{B})\varphi}\quad\text{for}\quad\varphi<\varphi', \tag{A4}$$

where the four coefficients can be determined by four conditions: two of them are the boundary conditions (A1) (where G_R and G_R' must be used for $\varphi=\pi$ and G_L and G_L' for $\varphi=-\pi$), and another two results from matching the functions G_R and G_L, as φ approaches φ' from right and left, respectively. An integration of (2.10) along a small interval that contains φ' provides these two matching conditions that are as follows: the continuity of G when $\varphi\to\varphi'$, or equivalently

$$G_R(\varphi',\varphi')=G_L(\varphi',\varphi'), \tag{A5}$$

and a discontinuity in the first derivative that is given by

$$\frac{\partial}{\partial\varphi}G_R(\varphi,\varphi')\bigg|_{\varphi\to\varphi'_+}-\ \frac{\partial}{\partial\varphi}G_L(\varphi,\varphi')\bigg|_{\varphi\to\varphi'_-}=1. \tag{A6}$$

Imposition then of (A1), (A5), and (A6) on (A3) and (A4) results in the final form (3.8) used in Sec. III.

APPENDIX B

A series method is presented here, alternative to the matching method of Sec. III, that can be used for determining both the wave functions and the energy spectrum, but only in the ordinary case $\theta=n\pi$. Direct substitution of (3.10) into (2.9) leads to a series representation of relative eigenfunctions, namely

$$\Phi(\varphi)=\frac{U}{2\pi}\sum_{n_1=-\infty}^{\infty}\frac{\exp\left[i\left(n_1-\frac{N}{2}\right)\varphi\right]\Phi(0)}{E-E^{(e)}_{n_1}-E^{(h)}_{N-n_1}}$$

with

$$E^{(e)}_{n_1}=\frac{\Delta}{2}(n_1-f)^2,\quad E^{(h)}_{N-n_1}=\frac{\Delta}{2}(N-n_1+f)^2 \tag{B1}$$

that can be transformed into

$$\Phi(\varphi)=-\Phi(0)\frac{U}{2\pi\Delta}e^{i(N/2)\varphi}\times\sum_{n_1=-\infty}^{\infty}\frac{e^{in_1\varphi}}{\left[n_1-\left(f+\frac{N}{2}\right)\right]^2-\left[\frac{E}{\Delta}-\frac{N^2}{4}\right]}. \tag{B2}$$

An exact summation result derived by contour integration, namely

$$\frac{1}{2\pi}\sum_{n_1=-\infty}^{\infty}\frac{e^{in\varphi}}{(n+A)^2-B}=\frac{1}{4\sqrt{B}}\left(\frac{e^{i(A-\sqrt{B})(-\varphi\pm\pi)}}{4\sqrt{B}\,\sin[\pi(A-\sqrt{B})]}-\frac{e^{i[(A+\sqrt{B})(-\varphi\pm\pi)]}}{4\sqrt{B}\,\sin[\pi(A+\sqrt{B})]}\right), \quad \text{(B3)}$$

with the upper signs holding for $\varphi\geqslant 0$ and the lower for $\varphi\leqslant 0$, can then be used to give all relative states in closed form. This is actually done in Sec. V [see Eq. (5.2)]. Even before determining the states, however, one can immediately derive the energy spectrum by considering the limit $\varphi\to 0$ in (B2). In this limit the sum (B3) yields

$$\begin{aligned}\frac{1}{2\pi}\sum_{n_1=-\infty}^{\infty}\frac{1}{(n+A)^2-B}&=\frac{1}{4\sqrt{B}}\{\cot[\pi(A-\sqrt{B})]-\cot[\pi(A+\sqrt{B})]\}\\&=-\frac{1}{2\sqrt{B}}\frac{\sin[2\pi\sqrt{B}]}{\cos[2\pi f+\pi N]-\cos[2\pi\sqrt{B}]},\end{aligned} \quad \text{(B4)}$$

which in combination with (B2), with

$$A=-\left(f+\frac{N}{2}\right),\quad B=\frac{E}{\Delta}-\frac{N^2}{4},$$

and after cancellation of the common factor $\Phi(0)$, leads to

$$\frac{\sin[2\pi\sqrt{B}]}{\cos[2\pi f+\pi N]-\cos[2\pi\sqrt{B}]}=\frac{2\Delta\sqrt{B}}{U}. \quad \text{(B5)}$$

This condition is shown in Sec. IV to be indeed equivalent to the energy spectrum condition (4.3) in the case of ordinary states.

APPENDIX C

We present here analytical expressions of various measurable quantities with the use of variables Φ_c and φ (and their combined variation shown in Fig. 2), that are essential for the arguments of Sec. VI. In particular, from (6.6) and transformation to the new variables, the probability density takes the form

$$\rho(\bar{\varphi})=\frac{1}{R}\int_{\bar{\varphi}-2\pi}^{\bar{\varphi}}d\varphi|\Phi(\varphi)|^2\left|\Psi_c\left(\bar{\varphi}-\frac{\varphi}{2}\right)\right|^2+\frac{1}{R}\int_{-\bar{\varphi}}^{2\pi-\bar{\varphi}}d\varphi|\Phi(\varphi)|^2\left|\Psi_c\left(\bar{\varphi}+\frac{\varphi}{2}\right)\right|^2 \quad \text{(C1)}$$

when integration with respect to Φ_c is carried out first, or equivalently

$$\rho(\bar{\varphi})=\frac{2}{R}\int_{\bar{\varphi}/2}^{(\bar{\varphi}/2)+\pi}d\Phi_c|\Psi_c(\Phi_c)|^2[|\Phi(2\bar{\varphi}-2\Phi_c)|^2+|\Phi(2\Phi_c-2\bar{\varphi})|^2] \quad \text{(C2)}$$

when integration with respect to φ is performed first. Similarly, for the probability current density we obtain

$$\begin{aligned}J(\bar{\varphi})=&\frac{i\hbar}{4mR^2}\int_{\bar{\varphi}-2\pi}^{\bar{\varphi}}d\varphi|\Phi(\varphi)|^2\left[\Psi_c\left(\bar{\varphi}-\frac{\varphi}{2}\right)\frac{\partial\Psi_c^*\left(\bar{\varphi}-\frac{\varphi}{2}\right)}{\partial\left(\bar{\varphi}-\frac{\varphi}{2}\right)}-\Psi_c^*\left(\bar{\varphi}-\frac{\varphi}{2}\right)\frac{\partial\Psi_c\left(\bar{\varphi}-\frac{\varphi}{2}\right)}{\partial\left(\bar{\varphi}-\frac{\varphi}{2}\right)}\right]+\frac{i\hbar}{2mR^2}\int_{\bar{\varphi}-2\pi}^{\bar{\varphi}}d\varphi\left|\Psi_c\left(\bar{\varphi}-\frac{\varphi}{2}\right)\right|^2\left[\Phi(\varphi)\frac{\partial\Phi^*(\varphi)}{\partial\varphi}-\Phi^*(\varphi)\frac{\partial\Phi(\varphi)}{\partial\varphi}\right]\\&-\frac{i\hbar}{2mR^2}\int_{-\bar{\varphi}}^{2\pi-\bar{\varphi}}d\varphi\left|\Psi_c\left(\bar{\varphi}+\frac{\varphi}{2}\right)\right|^2\left[\Phi(\varphi)\frac{\partial\Phi^*(\varphi)}{\partial\varphi}-\Phi^*(\varphi)\frac{\partial\Phi(\varphi)}{\partial\varphi}\right]\\&+\frac{i\hbar}{4mR^2}\int_{-\bar{\varphi}}^{2\pi-\bar{\varphi}}d\varphi|\Phi(\varphi)|^2\left[\Psi_c\left(\bar{\varphi}+\frac{\varphi}{2}\right)\frac{\partial\Psi_c^*\left(\bar{\varphi}+\frac{\varphi}{2}\right)}{\partial\left(\bar{\varphi}+\frac{\varphi}{2}\right)}-\Psi_c^*\left(\bar{\varphi}+\frac{\varphi}{2}\right)\frac{\partial\Psi_c\left(\bar{\varphi}+\frac{\varphi}{2}\right)}{\partial\left(\bar{\varphi}+\frac{\varphi}{2}\right)}\right]-\frac{\hbar}{mR}\frac{\Phi}{\Phi_0}\frac{\rho_{\mathrm{el}}(\bar{\varphi})}{e},\end{aligned} \quad \text{(C3)}$$

or equivalently,

$$J(\overline{\varphi}) = \frac{i\hbar}{2mR^2}\int_{\overline{\varphi}/2}^{(\overline{\varphi}/2)+\pi} d\Phi_c[|\Phi(2\overline{\varphi}-2\Phi_c)|^2+|\Phi(2\Phi_c-2\overline{\varphi})|^2]\left[\Psi_c(\Phi_c)\frac{\partial\Psi_c^*(\Phi_c)}{\partial\Phi_c}-\Psi_c^*(\Phi_c)\frac{\partial\Psi_c(\Phi_c)}{\partial\Phi_c}\right]$$
$$+\frac{i\hbar}{mR^2}\int_{\overline{\varphi}/2}^{(\overline{\varphi}/2)+\pi} d\Phi_c|\Psi_c(\Phi_c)|^2\left[\Phi(2\overline{\varphi}-2\Phi_c)\frac{\partial\Phi^*(2\overline{\varphi}-2\Phi_c)}{\partial(2\overline{\varphi}-2\Phi_c)}-\Phi^*(2\overline{\varphi}-2\Phi_c)\frac{\partial\Phi(2\overline{\varphi}-2\Phi_c)}{\partial(2\overline{\varphi}-2\Phi_c)}\right]$$
$$-\frac{i\hbar}{mR^2}\int_{\overline{\varphi}/2}^{(\overline{\varphi}/2)+\pi} d\Phi_c|\Psi_c(\Phi_c)|^2\left[\Phi(2\Phi_c-2\overline{\varphi})\frac{\partial\Phi^*(2\Phi_c-2\overline{\varphi})}{\partial(2\Phi_c-2\overline{\varphi})}-\Phi^*(2\Phi_c-2\overline{\varphi})\frac{\partial\Phi(2\Phi_c-2\overline{\varphi})}{\partial(2\Phi_c-2\overline{\varphi})}\right]-\frac{\hbar}{mR}\frac{\Phi}{\Phi_0}\frac{\rho_{\mathrm{el}}(\overline{\varphi})}{e}, \tag{C4}$$

and similar forms (but with a different structure of signs) result for ρ_{el} and J_{el} [see in particular Eq. (6.27)]. Such expressions lead to the possibility of symmetry breaking as discussed in the text.

*Corresponding author. Electronic address: cos@ucy.ac.cy

[1] A. V. Chaplik, JETP Lett. **62**, 900 (1995).
[2] A. B. Kalameĭtsev, V. M. Kovalen, and A. O. Govorov, JETP Lett. **68**, 669 (1998).
[3] R. A. Römer and M. E. Raikh, Phys. Rev. B **62**, 7045 (2000).
[4] J. Song and S. E. Ulloa, Phys. Rev. B **63**, 125302 (2001).
[5] H. Hu, J. L. Zhu, D. J. Li, and J. J. Xiong, Phys. Rev. B **63**, 195307 (2001).
[6] A. O. Govorov, S. E. Ulloa, K. Karrai, and R. J. Warburton, Phys. Rev. B **66**, 081309 (2002).
[7] A. V. Maslov and D. S. Citrin, Phys. Rev. B **67**, 121304 (2003).
[8] M. Bayer, M. Korkusinski, P. Hawrylak, T. Gutbrod, M. Michel, and A. Forchel, Phys. Rev. Lett. **90**, 186801 (2003).
[9] E. Ribeiro, A. O. Govorov, W. Carvalho, and G. Medeiros-Rebeiro, Phys. Rev. Lett. **92**, 126402 (2004).
[10] Y. Aharonov and D. Bohm, Phys. Rev. **115**, 485 (1959).
[11] M. Büttiker, Y. Imry, and R. Landauer, Phys. Lett. **96A**, 365 (1983).
[12] S. Washburn and R. A. Webb, Rep. Prog. Phys. **55**, 1311 (1992).
[13] Y. Imry, *Introduction to Mesoscopic Physics* (Oxford University Press, New York, 1997).
[14] M. V. Berry, Proc. R. Soc. London, Ser. A **392**, 45 (1984).
[15] N. Byers and C. N. Yang, Phys. Rev. Lett. **7**, 46 (1961).
[16] F. Bloch, Phys. Rev. Lett. **21**, 1241 (1968).
[17] A. Lorke, R. J. Luyken, A. O. Govorov, J. P. Kotthaus, J. M. Garcia, and P. M. Petroff, Phys. Rev. Lett. **84**, 2223 (2000).
[18] M. M. Nieto, Phys. Rev. A **61**, 034901 (2000).
[19] K. Moulopoulos and N. W. Ashcroft, Phys. Rev. B **48**, 11646 (1993).
[20] K. Moulopoulos and N. W. Ashcroft, Phys. Rev. B **42**, 7855 (1990).
[21] G. Vignale, Phys. Rev. B **51**, 2612 (1995).
[22] K. Moulopoulos and M. Constantinou (unpublished).
[23] G. Falci, R. Fazio, G. M. Palma, J. Siewert, and V. Vedral, Nature (London) **407**, 355 (2000).